

Article

Spatiotemporal Analytics of Environmental Sounds and Influencing Factors Based on Urban Sensor Network Data

Yanjie Zhao ^{1,†}, Jin Cheng ^{1,*}, Shaohua Wang ^{2,3,4,†} , Lei Qin ^{1,5,6} and Xueyan Zhang ⁷

¹ Beijing Key Laboratory for Sensor, School of Applied Sciences, Jianxiangqiao Campus, Beijing Information Science and Technology University, Beijing 100101, China; 2021021050@bistu.edu.cn (Y.Z.); qinlei@bistu.edu.cn (L.Q.)

² International Research Center of Big Data for Sustainable Development Goals, Beijing 100094, China; wangshaohua@aircas.ac.cn

³ State Key Laboratory of Remote Sensing Science, Aerospace Information Research Institute, Chinese Academy of Sciences, Beijing 100094, China

⁴ Key Laboratory of Digital Earth Science, Aerospace Information Research Institute, Chinese Academy of Sciences, Beijing 100094, China

⁵ Beijing Key Laboratory for Optoelectronic Measurement Technology, Beijing Information Science & Technology University, Beijing 100192, China

⁶ Key Laboratory of Modern Measurement & Control Technology, Ministry of Education, Beijing Information Science & Technology University, Beijing 100192, China

⁷ College of Letters and Science, University of California, Santa Barbara, CA 93106, USA; xueyan@ucsb.edu

* Correspondence: chengjin@bistu.edu.cn; Tel.: +86-10-6488-4673

† These authors contributed equally to this work.

Abstract: Urban construction has accelerated the deterioration of the urban sound environment, which has constrained urban development and harmed people's health. This study aims to explore the spatiotemporal patterns of environmental sound and determine the influencing factors on the spatial differentiation of sound, thus supporting sustainable urban planning and decision-making. Fine-grained sound data are used in most urban sound-related research, but such data are difficult to obtain. For this problem, this study analyzed sound trends using Array of Things (AoT) sensing data. Additionally, this study explored the influences on the spatial differentiation of sound using GeoDetector (version number: 1.0-4), thus addressing the limitation of previous studies that neglected to explore the influences on spatial heterogeneity. Our experimental results showed that sound levels in different areas of Chicago fluctuated irregularly over time. During the morning peak on weekdays: the four southern areas of Chicago have a high-high sound gathering mode, and the remaining areas are mostly randomly distributed; the sound level of a certain area has a significant negative correlation with population density, park area, and density of bike route; park area and population density are the main factors affecting the spatial heterogeneity of Chicago's sound; and population density and park area play an essential role in factor interaction. This study has some theoretical significance and practical value. Residents can choose areas with lower noise for leisure activities according to the noise map of this study. While planning urban development, urban planners should pay attention to the single and interactive effects of factors in the city, such as parks, road network structures, and points of interest, on the urban sound environment. Researchers can build on this study to conduct studies on larger time scales.



Citation: Zhao, Y.; Cheng, J.; Wang, S.; Qin, L.; Zhang, X. Spatiotemporal Analytics of Environmental Sounds and Influencing Factors Based on Urban Sensor Network Data. *ISPRS Int. J. Geo-Inf.* **2023**, *12*, 386. <https://doi.org/10.3390/ijgi12090386>

Academic Editors: Huayi Wu and Wolfgang Kainz

Received: 26 June 2023

Revised: 24 August 2023

Accepted: 15 September 2023

Published: 21 September 2023



Copyright: © 2023 by the authors. Licensee MDPI, Basel, Switzerland. This article is an open access article distributed under the terms and conditions of the Creative Commons Attribution (CC BY) license (<https://creativecommons.org/licenses/by/4.0/>).

Keywords: urban sound environment; spatiotemporal analytics; GeoDetector; influencing factors; sustainable development

1. Introduction

Urban sustainable development is affected by multiple factors, such as rising populations, climatic change, spatial planning, and the geographic distribution of building coverage [1,2]. Noise is an issue that runs through all the sustainable development goals [3].

Improvement of sound quality is beneficial to achieve the sustainable development goals, such as health and well-being, as well as quality education. Considering noise more in urban construction can reduce the economic losses caused by insufficient resources and reconstruction. A good sound environment is crucial to build a more sustainable city. Noise also reflects social inequality to a certain extent. Vulnerable groups are more susceptible to noise. Noise pollution has attracted widespread concern from all over the world and from all walks of life and has recently been the subject of much discussion and research among scholars. With the acceleration of urbanization and motorization, the environmental pressure brought by urban noise pollution is rising. Noise pollution has a remarkable negative impact on human health, such as hearing loss [4], mental health [5,6], sleep disorder [7], cardiovascular diseases [8], hypertension [9], and obesity [10]. In addition, noise can also adversely affect the reproduction and distribution of animals [11]. Therefore, it is essential to assess and analyse urban noise to support noise management.

Nowadays, various sensors are installed and deployed in cities to monitor diverse information inside the city, which has gradually become one of the trends in the development of smart cities. The Array of Things (AoT, see <https://arrayofthings.github.io/> (accessed on 11 January 2022)) project is a smart city measurement project designed to build city-scale sensor networks for understanding cities and urban life [12,13]. The AoT project deployed nodes with multiple sensors and cameras in the city of Chicago to collect near-real-time, location-based data on urban environments, infrastructure, and activities. The data measured by these nodes include light, temperature, vibration, sulfur dioxide, ozone, and sound intensity. About 130 nodes had been installed across Chicago by the end of January 2020. The dataset provided by the AoT has been widely used in various studies. The literature [14] studied the heat environment of Chicago based on CyberGIS-jupyter and temperature data provided by the AoT, and the study demonstrated the ability of CyberGIS-jupyter and AoT sensing data to support urban analysis. The literature [15] developed a framework by integrating CyberGIS and machine learning, which was utilized to make fine-grained spatiotemporal predictions of urban heat island in Chicago and achieved better results. The authors used AoT sensing data in the prediction process. The literature [16] combined AoT sensor data with family data of 450 elderly residents in Chicago to explore the health effects of air pollution using GIS and spatial modeling. All of the above studies have shown that the data have some research value. However, the results of our literature search indicate that there are few studies on the sound data provided by the AoT at present.

Noise monitoring and sound data mining are crucial prerequisites for urban noise management. Our study focuses on the analysis of urban sound spatiotemporal trends and the mining of sound influencing factors. Since the influence of natural and anthropogenic factors on the urban sound environment is a complex process, the acquisition of urban sound data is not an easy task. Therefore, there are three key challenges in the study of sound data. The first is the acquisition of sound data; the second is the delineation of discrete sound nodes over the study area; and the last is the selection of methods for analyzing urban sound influences. In this study, we propose to use the sound data provided by the AoT, divide the discrete sound nodes over the spatial region using Thiessen polygon, and utilize GeoDetector for the mining of sound influencing factors.

Taking Chicago as the study area, this study generated the noise maps of Chicago in the morning and evening peak on both weekdays and weekends based on the Thiessen polygon and the geographic information system. Using the statistical method of spatial correlation analysis and GeoDetector, we studied the spatiotemporal distribution characteristics of Chicago's sound. In addition, we discussed the impacts of seven factors and the interaction between these factors on the spatial variation of Chicago's sound. The factors include the population density, park area, density of the road network, density of the sidewalk, density of bike routes, number of hospitals, and number of fire stations. This study expects to support urban planning and policy-making and have positive significance for the sustainable development of Chicago by providing reference value to some extent. This

paper is divided into seven aspects as follows. Following the description of the introduction in Section 1 and the relevant research on the topic of sound in Section 2, Section 3 describes the research area and the data source. Section 4 presents the experiment methods, including Thiessen polygon and GeoDetector. Section 5 illustrates the noise maps and explains the experimental results. Section 6 discusses the experimental results combining a correlation analysis and GeoDetector. Section 7 concludes this study.

2. Related Work

Experts and scholars have studied the topic of the urban sound environment with various acquisition and analysis methods of sound data. The literature [17] designed an environmental health monitoring program that users can use to measure their noise exposure continuously and mark the sound. The literature [18] created a noise map of New York City based on complaints data, social media, road networks, and Point of Interest (POIs), mainly illustrating location ranks according to the value of noise indicators and displaying noise distribution of different noise categories. These studies focus on the composition or distribution of noise and methods to obtain better noise data. These studies focus on fine-grained data, such as how each noise may be associated with location, timestamp, and fine-grained noise categories, such as noisy music or construction noise. However, it is difficult and costly to obtain fine-grained data. The sound data provided by AoT are time series data, with an acquisition interval of the 20 s. Compared with the fine-grained data, the AoT dataset is freely accessible and has smaller temporal granularity.

Leisure activities associated with various high-power sound systems, celebrations, and transportation are partial sources of urban noise [19]. Road traffic noise is the most important source of environmental noise [20], but the green belt along roads effectively mitigates traffic-induced noise pollution [21,22]. As the vegetation density on both sides of the road changes from sparse to moderate, traffic noise can be significantly reduced [23]. In addition, building density and land use type also affect urban noise levels [24,25]. The literature [26] analyzed the impact of human activities on noise complaint behavior by combining the spatial distribution characteristics of POIs and found that there is a certain correlation between noise complaints and the distribution and types of POIs. The POIs they selected included 14 types of data, such as scenic spots, public facilities, transportation facilities, and medical care. The literature [27] realized the assessment of people exposed to traffic noise in the main urban area of Guangzhou based on POIs and noise maps, and the study found that areas with higher population density are affected by traffic noise more, and usually areas with POI types of residential, catering services, shopping services, and living services are densely populated. The literature [25] explored the relationship between urban noise and socio-economic factors, such as population and nighttime light intensity; explored the impact of landscape structure on urban noise; and studied the impact of different urban forms on urban noise based on urban functional areas. Their study found that urban vegetation can reduce urban environmental noise, and road density aggravates urban environmental pollution. From this, it is easy to find that the factors often used by researchers in urban noise analysis include population, vegetation, traffic, and buildings, and when considering traffic, more consideration is given to the road network for motor vehicles, and sidewalks and bicycle paths are seldom considered separately. In addition, researchers' selection of factors is coarse-grained. Coarse-grained factors often cause us to overlook certain implications of finer-grained factors. Therefore, in our study, seven factors—population, parks, road network, sidewalks, bike lanes, fire stations, and hospitals—were selected to explore the impact of these factors on Chicago's sound. The selection of fine-grained factors is novel to the current study.

Geographic Information Systems (GIS) are often used in urban noise analysis, especially in the drawing of urban noise maps. Past studies have demonstrated the effectiveness and importance of using GIS in noise analysis [28,29]. The noise map can intuitively reflect the distribution of noise, which is conducive to noise assessment. The literature [30] drew a dynamic traffic noise map using noise monitoring data and traffic speed data. The litera-

ture [31] drew a 24-h noise map of Chancheng District in Foshan, China. The study [29] used GIS and GPS to map daytime and nighttime traffic noise in Guangzhou, China. The literature [32] created a noise map of Şanlıurfa using GIS. We can find that noise maps have become one of the effective methods for reflecting noise levels. These studies provide us with ideas for noise mapping. When studying a phenomenon, the driving factors are usually explored. A commonly used driver analysis method is geographically weighted regression (GWR) [33]. The GWR has been widely used in various studies, such as the spatial distribution of Tibetan Buddhist Monasteries [34], the spatial–temporal distribution of PM_{2.5} [35], and the spatial–temporal analysis of rock concerts [36]. However, as with other regression analysis techniques, the GWR method suffers from the problem of multicollinearity, and the results of the analysis can be easily influenced by it. Currently, GeoDetector has been widely used as a powerful tool for driver and factor analysis in a variety of fields: agriculture [37], plants [38,39], geology [40], pollution [41,42], tourism [43], health [44], etc. GeoDetector is a statistical method that detects the spatial heterogeneity of geographic phenomena to reveal the driving forces behind it [45,46]. Its core idea is that if an independent variable has an important influence on a dependent variable, the spatial distribution of the independent variable and the dependent variable should be similar. Compared with other methods of driving factor analysis, GeoDetector is more suitable for processing geographical data [47].

3. Research Area and Data

In our study, we choose Chicago as the research area, as shown in Figure 1. Chicago is the third largest economy in the US and one of the world's international financial centres, which is at the crossroads of North American rail, road, and air transport infrastructure, accounting for about 28,000 km² with the population more than 10 million in the region [14]. Additionally, the existing studies have revealed that Chicago's environmental noise level is high enough to be problematic [48].

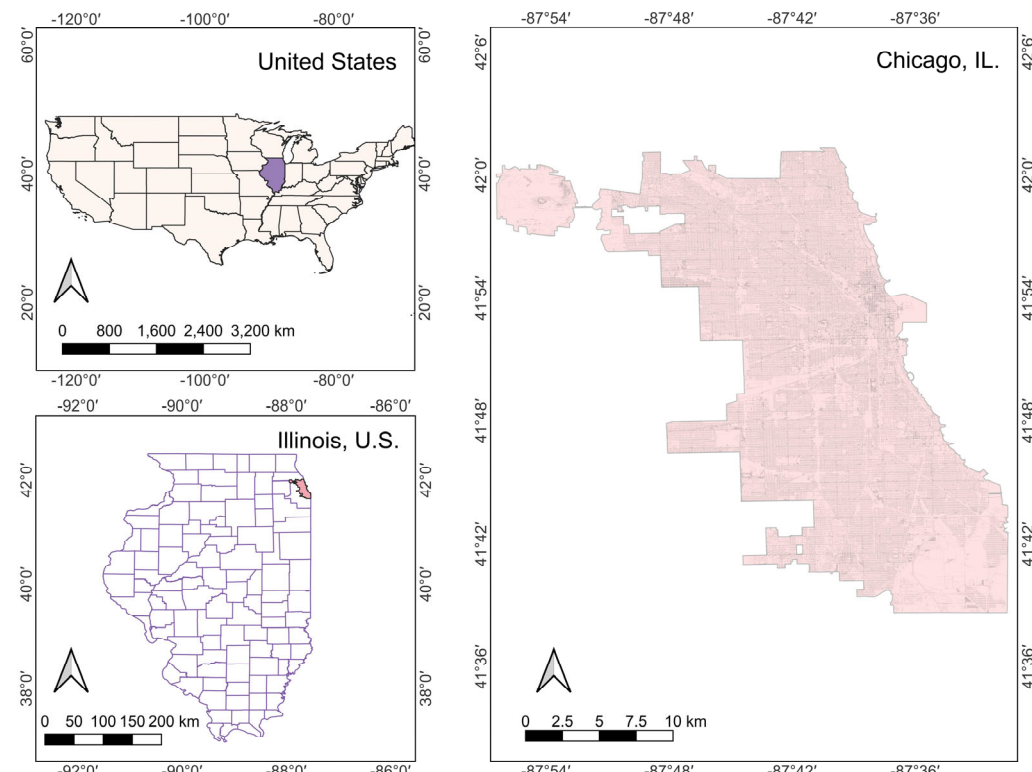


Figure 1. Study area.

The data provided by AoT includes 4 datasets (Table 1), namely data dataset, node dataset, sensor dataset, and provenance dataset. Each dataset is a csv file. This study mainly uses data dataset and node dataset in AoT. The data dataset describes the measured values of the object at each time point during a certain period, see Table 2 for details. The node dataset mainly comprises node descriptions, see Table 3 for details. The sound data in our study comes from AoT data in Chicago from 30 September 2019 to 6 October 2019. There are 126 nodes in these data, including 36 sound nodes. Among the 36 sound nodes, one node is working abnormally, and the monitored sound level is NA. The spatial distribution of these nodes in Chicago is shown in Figure 2. Sound nodes that work normally are orange, black nodes represent abnormal sound nodes, and blue nodes are all nodes except sound nodes distributed in Chicago. In addition, the sound data contained in these data can be obtained by specifying the sensor. The sensor for acquiring sound data is spv1840lr5h_b.

Table 1. Description of the dataset provided by AoT.

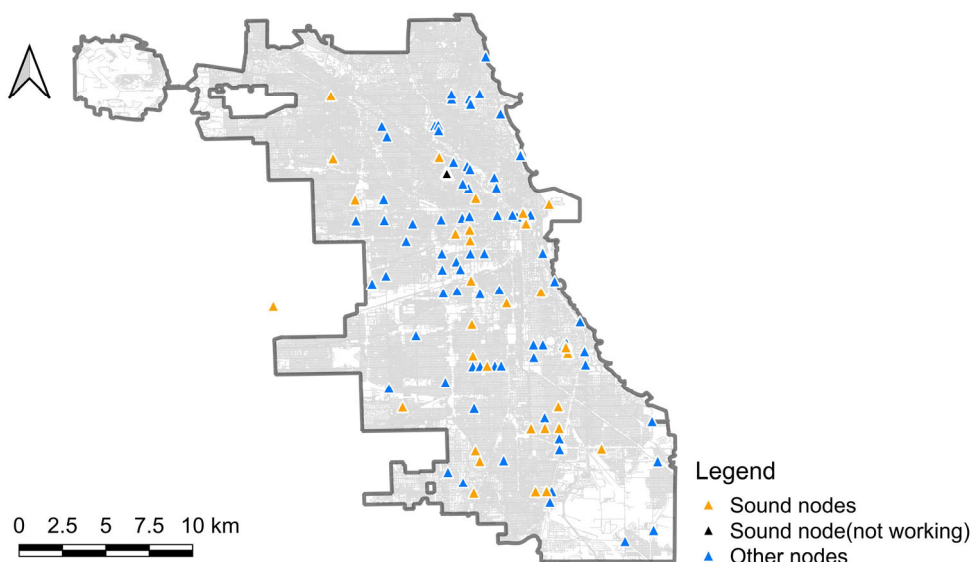
Dataset	Description	Content
data.csv	Sensor data ordered by ascending timestamp	Describe the measurement completed time by UTC timestamp, take the measurement of ID of nodes, measured sensor name, measured sensor parameter, original value read from sensor, and converted “human readable” value from sensor.
node.csv	Node metadata	Node ID, project ID of managed node, node public name, node installed street address, node installation latitude, node installation longitude, detailed description of node’s build and configuration, node installation starting timestamp, node installation ending timestamp.
sensors.csv	Sensor metadata	Ontology of measurement, subsystem containing sensor, sensor name, sensor parameter, physical units of HRF value, minimum HRF value according to datasheet (used as lower bound in range filter), maximum HRF value according to datasheet (used as upper bound in range filter), reference to sensor’s datasheet.
provenance.csv	Provenance metadata	Data format version, project ID, minimum possible publishing UTC timestamp, maximum possible publishing UTC timestamp, UTC timestamp of this digest was created, URL where this digest was provided.

Table 2. List of data formats of the dataset.

Timestamp	Node_ID	Subsystem	Sensor	Parameter	Value_Raw	Value_Hrf
30 September 2019 00:00:02	001e0610f703	lightsense	apds_9006_020	intensity	28	2.251
30 September 2019 00:00:06	001e0610f6db	chemsense	at0	temperature	2204.0	22.04
30 September 2019 00:00:07	001e0610ba46	lightsense	hih6130	humidity	11096	67.73
30 September 2019 00:00:08	001e0610f732	lightsense	hmc5883l	magnetic_field_x	-118	-107.273
30 September 2019 00:00:09	001e0610ba15	metsense	bmp180	pressure	10,551,296	984.02
30 September 2019 00:00:10	001e061144be	chemsense	co	concentration	3414.0	-1.46383
30 September 2019 00:00:12	001e06113107	metsense	spv1840lr5h_b	intensity	NA	56.72

Table 3. List of data formats of node dataset.

Node_ID	Project_ID	Vsn	Address	Lat	Lon	Description
001e0610ba46	AoT_Chicago	004	State St. & Jackson Blvd, Chicago, IL, USA	41.878377	-87.627678	AoT Chicago (S) [C]
001e0610ba3b	AoT_Chicago	006	18th St. & Lake Shore Dr., Chicago, IL, USA	41.858136	-87.616055	AoT Chicago (S)
001e061135cb	AoT_Chicago	052	Ashland & 63rd St., Chicago, IL, USA	41.779369	-87.66442099999998	AoT Chicago (S) [C]
001e0610ba8f	AoT_Chicago	00D	Cornell & 47th St., Chicago, IL, USA	41.810342	-87.590228	AoT Chicago (S)
001e0610bc10	AoT_Chicago	01F	State St. & 87th, Chicago, IL, USA	41.736314	-87.624179	AoT Chicago (S) [C]

**Figure 2.** Spatial distribution for AoT nodes in Chicago.

The influencing factors we selected in this study have seven factors, including population density (PD), park area (PA), density of road network (DRN), density of sidewalk (DS), density of bike route (DBR), number of hospitals (NH), and number of fire stations (NFS). See Table 4 for details.

Table 4. Factors selected for analysis.

Factor	Source
Population density (PD)	https://landscan.ornl.gov/ (accessed on 21 May 2022)
Park area (PA)	https://data.cityofchicago.org/Parks-Recreation/Parks-Chicago-Park-District-Park-Boundaries-current/ej32-qgdr (accessed on 21 May 2022)
Density of road network (DRN)	https://data.cityofchicago.org/Transportation/Street-Center-Lines/6imu-mieu (accessed on 29 May 2022)
Density of sidewalk (DS)	https://data.cityofchicago.org/Transportation/Sidewalks/77cn-6x4c (accessed on 29 May 2022)
Density of bike route (DBR)	https://data.cityofchicago.org/Transportation/Bike-Routes/3w5d-sru8 (accessed on 29 May 2022)
Number of hospitals (NH)	https://data.cityofchicago.org/Health-Human-Services/Hospitals-Chicago/ucpz-2r55 (accessed on 21 May 2022)
Number of fire stations (NFS)	https://data.cityofchicago.org/Public-Safety/Fire-Stations/28km-gtjn (accessed on 21 May 2022)

4. Methodology

4.1. Workflow

The experimental data provided by AoT and the seven factors, including PD, PA, DRN, DS, DBR, NH, and NFS in Chicago, were downloaded through the real-time API. The shapefile containing the geolocation information and the Chicago boundary was also obtained. The datasets were stored and managed consistent with the AoT data formats in the MySQL database (version number: 8.0.27) to facilitate data viewing, statistics, and processing. Statistics were performed to process missing and extreme values. Then, we plotted line charts that could reflect the trend of sound changes at different nodes. Noise maps in different time groups were drawn based on the Thiessen polygon method. Spatial correlations were analyzed using Moran's I . The effect of factors in the city on sound levels was analyzed using GeoDetector. Finally, the features of sound distribution and its influencing factors in Chicago regarding the analysis results were concluded. Figure 3 shows the workflow for exploring the spatiotemporal trends and influencing factors of Chicago sounds using AoT sensing data.

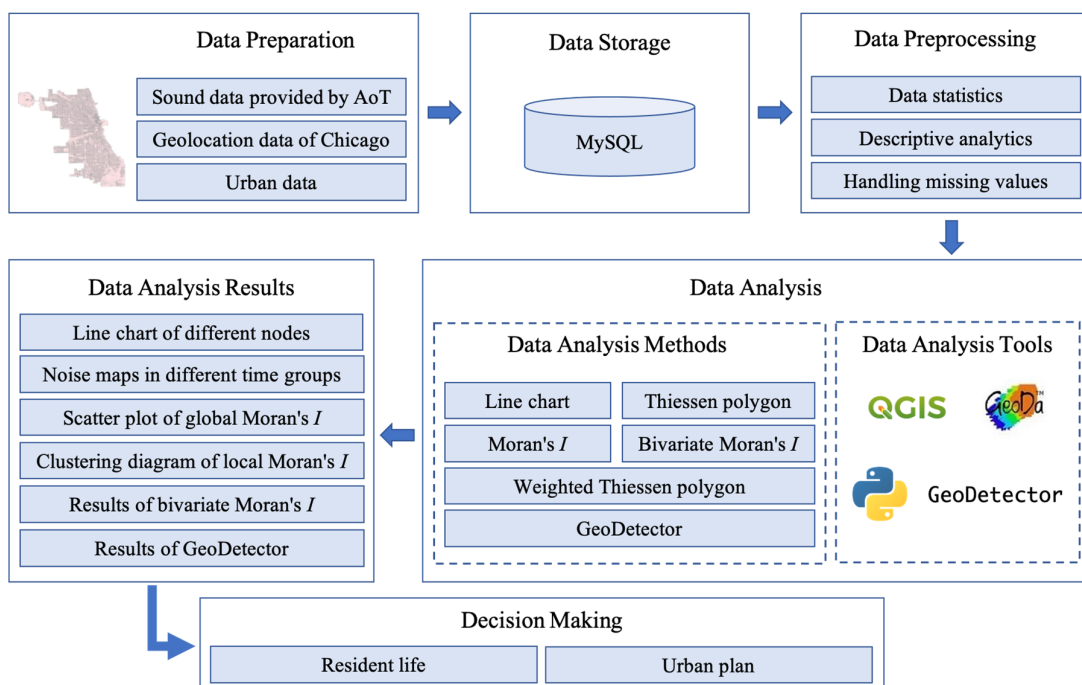


Figure 3. The workflow of environmental sounds analysis.

4.2. Data Processing of Sound Sensor

Our study focused on the sound data of Chicago from 30 September 2019 to 6 October 2019 with a total of 709,644 pieces, of which 2046 pieces were abnormal (the sound level was NA). Considering the relatively small proportion of missing values in the dataset, the samples with missing values were deleted, and the 707,598 pieces of sound data after deleting the abnormal data were analysed. Since a sound node worked abnormally and the 2046 pieces of data provided by this node were NA, the remaining 35 nodes participated in the analysis.

4.3. Thiessen Polygon

A·H·Thiessen proposed a method to calculate the average rainfall according to the rainfall measurements at discretely distributed meteorological stations, which is called the Thiessen polygon [49]. Thiessen polygon is composed of several polygons, and the rainfall intensity in a polygon is represented by the rainfall measured at the only weather station contained in the polygon. Thiessen polygon is characterized by three features:

(1) each polygon has only one discrete point; (2) points within a polygon are closest to the corresponding discrete point; and (3) points located on the sides of a polygon are equidistant from the discrete points on its two sides.

Thiessen polygons have a wide range of applications in practical problems. The study [50] divided the transit traffic analysis area based on the Thiessen polygon; the authors drew a conclusion that this division method is more in line with the actual situation of transit travel by combining the characteristics of Thiessen polygon and the transit travel. The main reason is that under this division method, each transit traffic analysis zone contains one transit stop, and each transit traffic analysis zone covers all the area between any two transit stops, which can meet the travel demand in the study area. The study [51] constructed a sewer model by drawing Thiessen polygon for sewer nodes and evaluated the model using the U.S. Environmental Protection Agency's stormwater management model. The study proved that Thiessen polygon can be used to construct urban stormwater models. Another study in the literature [52] focused on predicting the sales area of convenience stores. The method used by the authors in this study to classify the area covered by each convenience store as a neighbourhood is the Thiessen polygon, in which each polygon generated represents the area of influence of the convenience store, with only one convenience store per polygon and with any location within the polygon being closer to its convenience store than to any other convenience store. By overlaying the generated Thiessen polygons with 41 factors, such as bus stops, hospitals, banks, parks, fire stations, hypermarkets, and population, the influence of these factors on convenience store location was explored.

In our study, 35 sound monitoring regions were generated using Thiessen polygon for 35 sound nodes, and the sound intensity of each node was used to represent the sound intensity of the region where the node was located. The process of building Thiessen polygon is shown in Figure 4. In Figure 4, the blue points represent sound nodes. Each sound node corresponded to a polygon. The polygons of each sound node form the entire Thiessen polygon. The center of mass of the sound monitoring region was the node that monitors the sound, which was in line with the characteristics of sound sensors monitoring sound. Different colors of the polygon represent different sound levels.

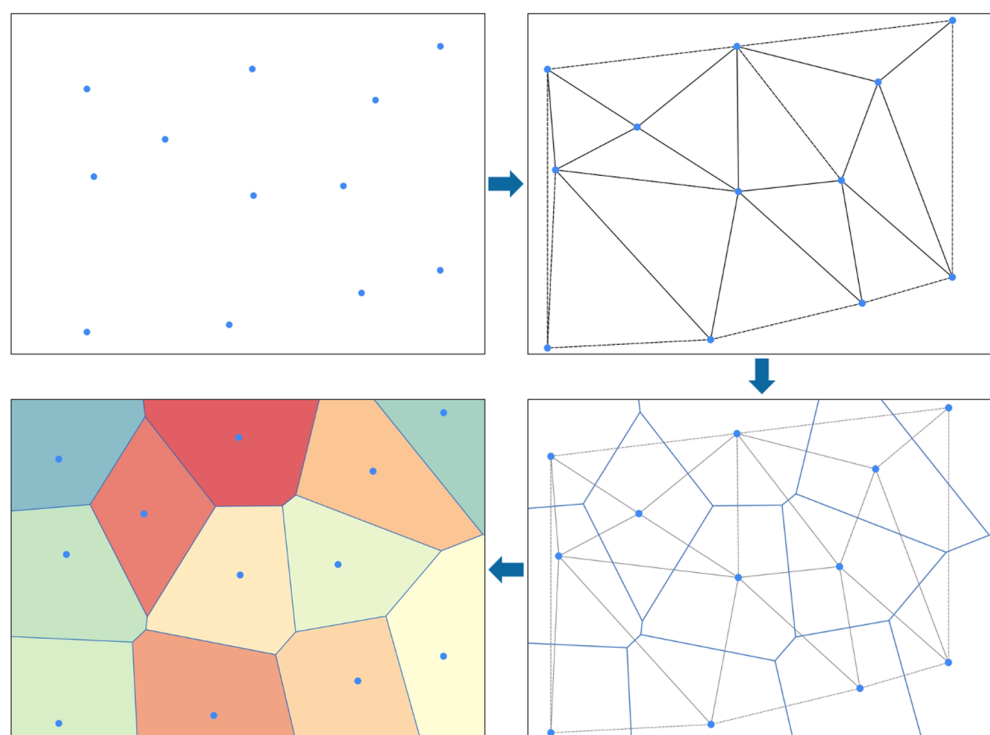


Figure 4. The establishment process of Thiessen polygon.

4.4. GeoDetector

Our study used a factor detector and an interactive detector in GeoDetector. The factor detector was used to explore the explanatory power of each influential factor on the spatial differentiation of Chicago sounds. The interaction detector was used to evaluate the impact type and intensity of the interaction between the two factors on the spatial differentiation of Chicago sounds. Since the factors we studied were numerical quantities, we utilized the GeoDetector with R package for analysis, supporting the selection of reasonable classification methods and classification intervals to discretize numerical quantities into type quantities. The formula for calculating the q value is:

$$q = 1 - \frac{\sum_{m=1}^P N_m \sigma_m^2}{N \sigma^2}, \quad (1)$$

where $m = 1, \dots, P$ is the stratification of factor X. N_m is the number of units in layer m . N is the number of units in the study area. σ_m^2 and σ^2 are the variance of layer m and the variance of the whole study area, respectively. q is the influence of the factors on the spatial differentiation of Chicago sounds, and the range of q value is $[0, 1]$. The larger the q value, the greater the influence of the factor on the spatial differentiation of Chicago sounds.

5. Experiment and Results

This study uses Anaconda to draw the trend graph of the noise levels at different nodes and perform a descriptive analysis of the data. In addition, the GIS software Quantum GIS (version number: 3.18) will complete the drawing of the Thiessen polygon and noise maps as well as the overlay of associated data. PyCharm (version number: 2019.1) realizes the drawing of a weighted Thiessen polygon, and GeoDa (version number: 1.20.0.8) completes spatial correlation analysis. The GeoDetector (R package) was used to explore the interpretation of different factors and the interaction of two factors on the sound changes in Chicago. Refer to https://github.com/HGISX/Chicago_Analytics_AOT (accessed on 21 May 2022) for relevant data and processing results.

5.1. Noise Level of Different Nodes

We drew a line graph of 35 nodes from 30 September 2019 to 6 October 2019 and analysed the trend of sound level changes at each node within a week. These line graphs are divided into four categories according to the trend of sound level (Refer to Appendices A–D for details), and the most representative nodes in each category are selected for analysis. In Figure 5A, there is a node that has a higher noise level throughout the week, and the overall noise level is higher than all other nodes. Among them, noise above 80.0 dB accounts for more than 76%, and noise above 90.0 dB accounts for more than 49%. Figure 5B represents 13 nodes in total. Despite the noise of the nodes being between 55.0 dB and 65.0 dB many times throughout the week, there were still several occasions when the noise was between 65.0 dB and 75.0 dB. There are 14 nodes represented in Figure 5C, and the noise of the nodes was between 55.0 dB and 65.0 dB most of the week, and sometimes, the noise exceeded 65.0 dB. Figure 5D shows a total of seven nodes, and the node data were seriously missing, but its overall noise was between 55.0 dB and 67.5 dB.

We can know from Figure 5 that the noise level of a node was generally much higher than that of other nodes compared with the other 34 nodes after analysing the noise trend of each node within the week. The common characteristic of these 35 nodes is that the noise level fluctuates irregularly over time.

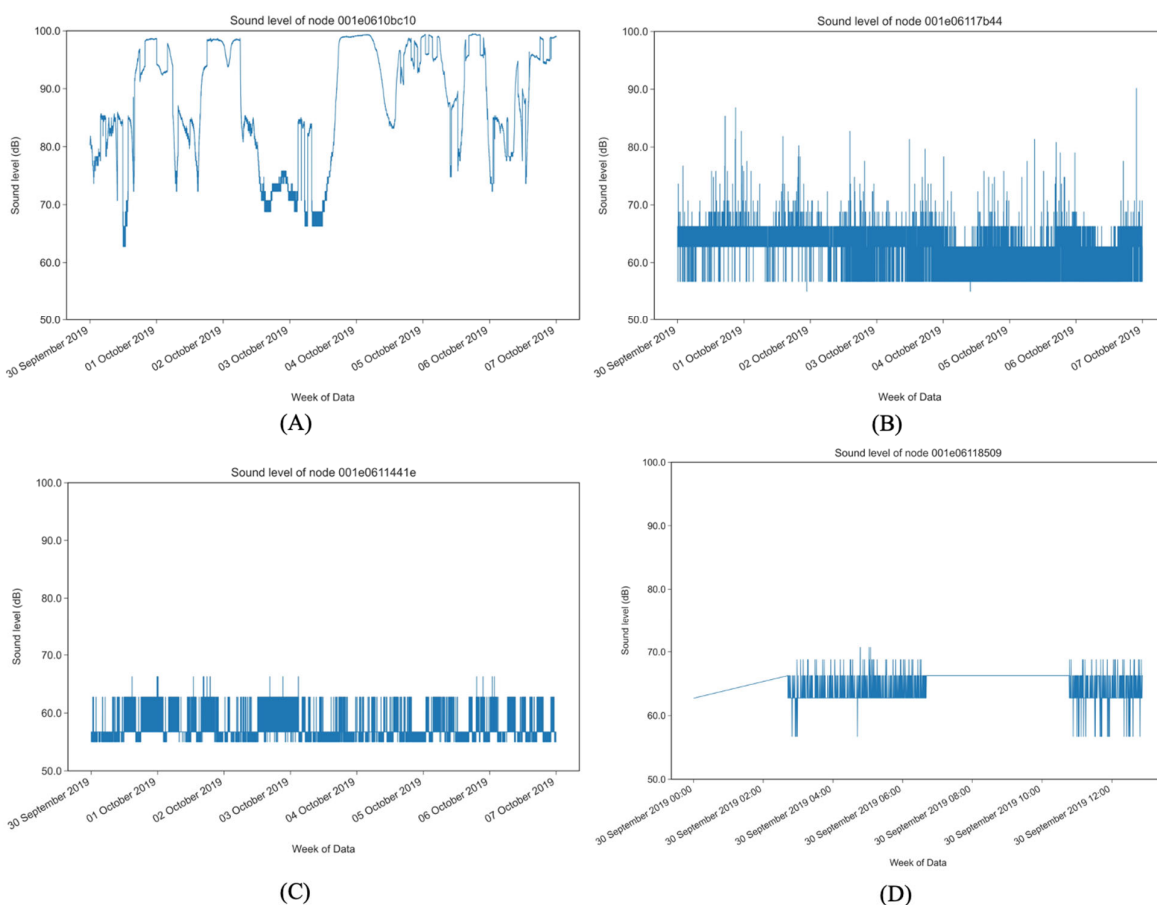


Figure 5. Noise level of (A) node 001e0610bc10; (B) node 001e06117b44; (C) node 001e0611441e; (D) node 001e06118509.

5.2. Noise Level on Weekdays and Weekends

To make full use of light resources and thus save energy, more than 70 countries, including the United States, have adopted Daylight Saving Time (DST) [53]. DST alters the clock such that in the spring, summer, and early autumn, sunset and sunrise are one hour later [54]. DST affects sleep and wellness in addition to morning and evening peak. According to the related DST research on traffic accidents in the US, it can be inferred that the morning peak is 4:00–9:00 a.m. and the evening peak is 4:00–9:00 p.m. during DST in the US [53–55].

Table 5 shows the noise statistics at morning and evening peak on weekdays and weekends in Chicago. It can be seen from Table 5 that the average noise level in the morning peak on weekdays is higher than that on weekends. According to the World Health Organization's Community Noise Guidelines [56], an average noise level of 55.0 dB would be troublesome; however, the average noise level in Chicago during the morning and evening peaks is over 59.0 dB, indicating some impact on Chicago residents. Secondly, the maximum noise level in the morning and evening peaks on weekdays and weekends exceeds 99.0 dB. According to World Health Organization guidelines, hearing damage may occur when the maximum noise level approaches 110.0 dB. Furthermore, the mean values of sound levels are greater than the median in different time groups. Although the average value of two for the evening peak sound conditions on weekdays and weekends is the same, the noise in the evening peak varies significantly on weekends. In addition, the average noise level in the evening peak on weekdays and weekends is slightly higher than that of the morning peak, which may be inseparable from the entertainment that people have at the end of the day.

Table 5. Sound statistics in different time groups.

		Mean (dB)	Std	Min (dB)	25% (dB)	50% (dB)	75% (dB)	Max (dB)
Weekday	Morning peak	59.6	6.4	55.0	56.7	56.7	62.7	99.3
	Evening peak	59.7	7.0	55.0	56.7	56.7	62.7	99.1
Weekend	Morning peak	59.4	6.4	55.0	56.7	56.7	62.7	99.1
	Evening peak	59.7	8.0	55.0	56.7	56.7	62.7	99.5

Some scholars often deal with layers in their research by adopting a superposition analysis to obtain the spatial potential information. The study [57] took this method for studying the noise of New York City. In their research, a map segmentation algorithm was used to divide New York into disjoint areas based on main roads, and then, the noise complaint data were mapped to their geographical location for analysis. In this study, 35 nodes are isolated on the map. The Thiessen polygon is first used to split Chicago into disjoint areas based on various positions of 35 nodes to make the analysis results general. The division results are shown in Figure 6. Then, the sound data are mapped to these areas according to their geographical position to complete the drawing of the noise maps, as shown in Figure 7. During the study, the average noise level of each node is used to represent the overall noise level of the area where the node is located.

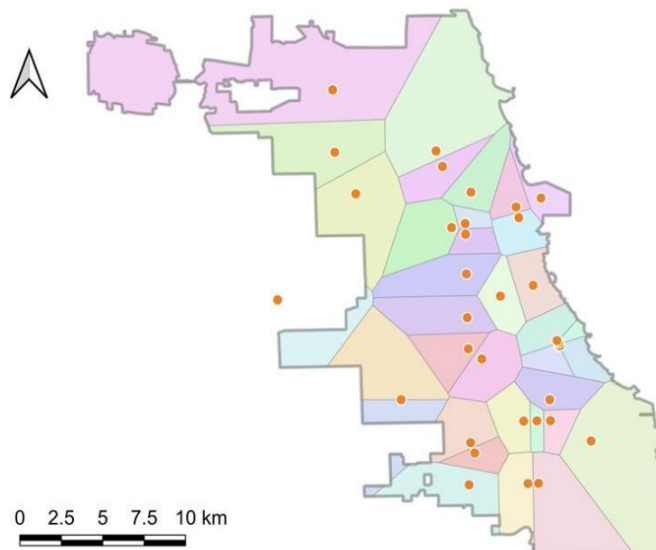
**Figure 6.** Partition based on Thiessen polygon.

Figure 7A shows the noise levels in different regions of Chicago during weekday morning peak hours, with a noise level between 85.0 dB and 90.0 dB, 11 areas between 60.0 dB and 65.0 dB, and 23 areas between 55.0 dB and 60.0 dB. Figure 7B displays the noise levels of various areas during weekend morning peak hours in Chicago, with a noise level between 85.0 dB and 90.0 dB, 10 areas between 60.0 dB and 65.0 dB, and 20 areas between 55.0 dB and 60.0 dB. In addition, there are four areas with no noise data during this period, which are 001e0610ee5d, 001e0611536c, 001e06118509, and 001e06182a7. Figure 7C indicates the noise levels of different areas of Chicago during weekdays evening peak hours, with a noise level between 90.0 dB and 95.0 dB, 8 areas between 60.0 dB and 65.0 dB, and 24 areas between 55.0 dB and 60.0 dB. Additionally, there are two areas with no noise data during this period, which are 001e0611850f and 001e06118509. Figure 7D depicts the noise levels of different zones during weekends evening peak hours in Chicago, with a noise level between 95.0 dB and 100.0 dB, 9 areas between 60.0 dB and 65.0 dB, and 21 areas between 55.0 dB and 60.0 dB. In addition, there are four areas with no noise data during this period, which are 001e0610ee5d, 001e0611536c, 001e06118509, and 001e06182a7.

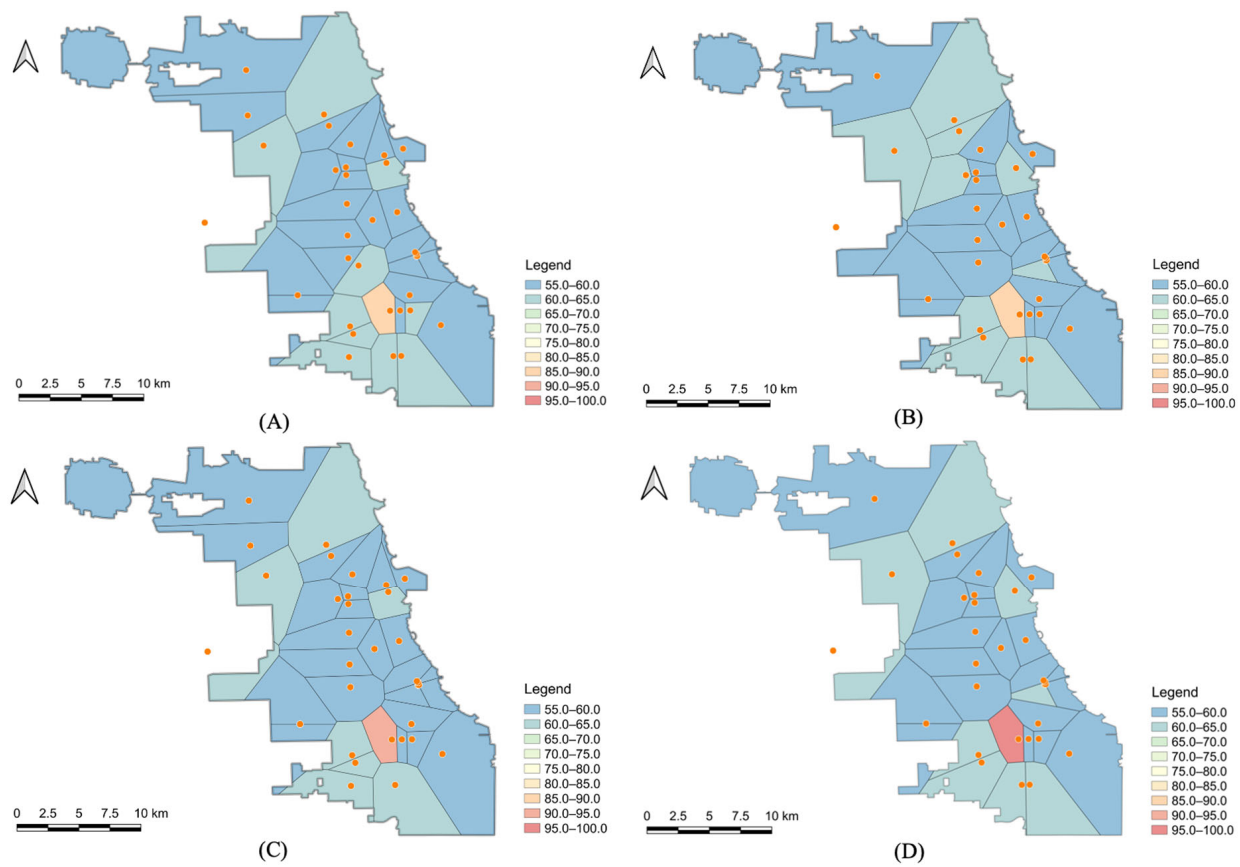


Figure 7. Noise level maps at (A) morning peak on weekdays; (B) morning peak on weekends; (C) evening peak on weekdays; and (D) evening peak on weekends (unit: dB).

It can be known from the noise maps that whether it is the morning peak and evening peak on weekdays or on weekends and that the noise level in most areas of Chicago is between 55.0 dB and 60.0 dB, few areas are between 60.0 dB and 65.0 dB, and only one area exceeds 85.0 dB. In addition, comparing Figure 7A,B, we can find that the overall noise level of the morning peak on weekdays is not much different from the overall noise level of the morning peak on weekends. After comparing Figure 7C,D, we can see that the noise level in the evening peak on weekdays is slightly lower than that in the evening peak on weekends.

The shape of the general Thiessen polygon completely depends on the position of sample data points and does not reflect the attribute difference of points [49]. Because of the disadvantages of singleness and equality in the selection of influencing factors, the general Thiessen polygon may not meet the complex realistic environment. Therefore, weight is introduced for each sound node. Considering the characteristics of the area where each node is located and taking the noise-generating ability of that area as a weighting factor, the weighted Thiessen polygon can be obtained [58]. As shown in Figure 8, a weighted Thiessen polygon helps to accurately describe the spatial extent and intensity of sound on a spatial scale. Figure 8 shows that the weighted Thiessen polygon presents different spatial patterns compared to the general Thiessen polygon.

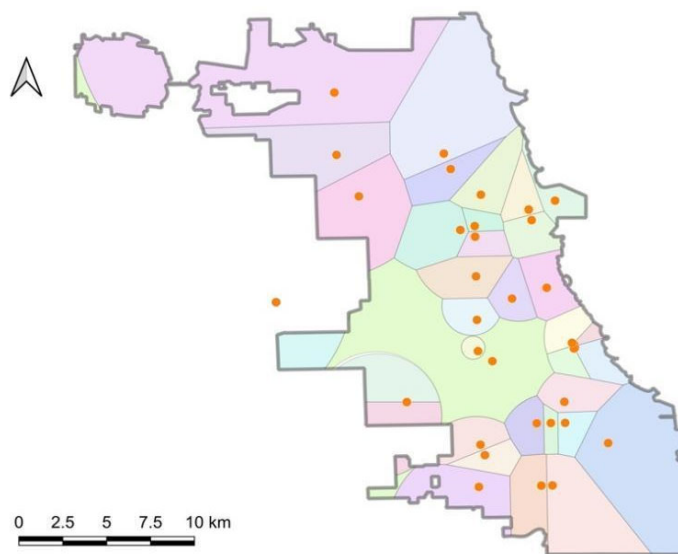


Figure 8. Partition based on weighted Thiessen polygon.

6. Discussion

Geographic objects form various spatial distribution patterns according to their attributes or human activities. Moran's I is widely used to quantify the level of spatial autocorrelation between adjacent locations, and the positive or negative value of Moran's I indicates that observations at locations that are spatially close tend to have identical or different values [59]. In this study, we attempted to perform spatial data analysis to explore spatial patterns of the noise level in Chicago. First, Moran's I at global and local scales was simulated based on observations (35 for weekday morning peak, 33 for weekday evening peak, 31 for morning and evening peaks on weekends). Figure 9 reveals a global Moran scatter plot of Chicago's noise for different time groups, and the sound level is used to represent the noise level. The Moran statistic for the morning peak on weekdays is 0.106, and the p -value is less than 0.05; that for the evening peak on weekdays is 0.068, and the p -value is less than 0.05, indicating that the spatial autocorrelation of Chicago's noise is statistical for two time groups (See Figure 9). Figure 10 displays a local Moran index cluster plot of Chicago's noise. High–high or low–low suggests that areas with high (low) noise are adjacent to other regions with high (low) noise. Whereas high–low or low–high states that areas with high (low) noise are adjacent to areas with low (high) noise. We may observe that the four southern areas of Chicago have a high–high sound gathering mode, and the remaining areas are mostly randomly distributed during the morning peak on weekdays. The difference from the morning peak on weekdays is that the two eastern regions of Chicago present a low–low sound gathering mode. Chicago sounds have different aggregation patterns in different time periods, which may be related to the different behavioral activities of people in these periods.

Correlations can be explored using multi-source data and spatial analysis methods [60]. Taking the morning peak on weekdays as an example, we examined the impact of PD, PA, DRN, DS, DBR, NH, and NFS on the sound environment through the bivariate Moran's I . We discovered that noise level in an area during the weekdays' morning peak was negatively correlated with the area's PD, PA, and DBR, and the correlation coefficients were 0.15 ($p < 0.01$), 0.18 ($p < 0.01$), and 0.10 ($p < 0.1$), respectively (Table 6). According to the analysis, we can know that: (1) the larger the population, the lower the noise. This may be connected to the location of people's activities, such as office buildings and residential buildings, and even if the population is large, there will be no excessive noise in general. (2) Areas with large park boundaries may have lower noise levels, and as parks continue to expand, noise levels decrease. This could be the case since the natural landscape features of the park, such as vegetation and water bodies, might affect the sound environment, and these impacts will increase along with the rising land area. This finding is identical to

existing results [61]. (3) With the increase of bike routes, the noise will be reduced. Cyclists are more likely to be exposed to noise in the short term, but with the increase in bike routes and the substitution of bicycles for cars and motorcycles, noise pollution will gradually decrease, and the noise pollution suffered by cyclists will also decrease [62]. Furthermore, we also found that there are no statistically significant correlations between the DS, DRN, NH, and NFS and the noise level, which may be because the impact of these factors on noise is an interactive and complex process.

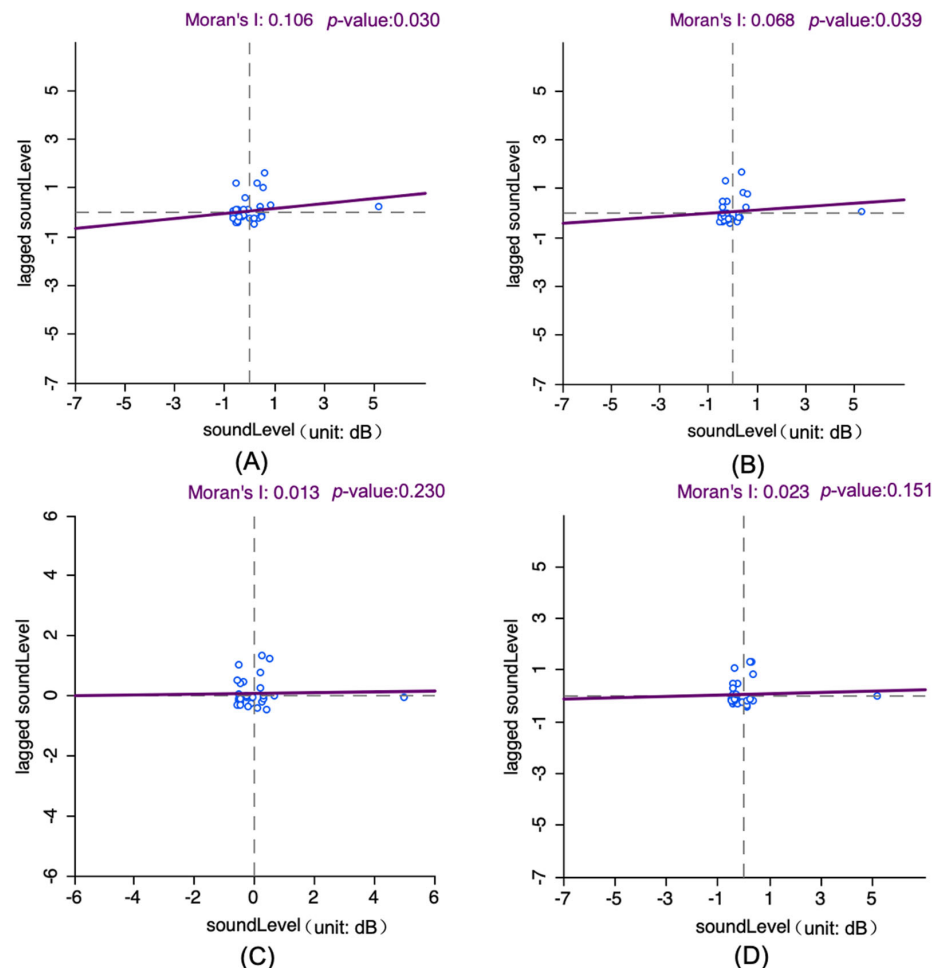


Figure 9. Scatter plot of global Moran's I : (A) morning peak on weekdays; (B) evening peak on weekdays; (C) morning peak on weekends; (D) evening peak on weekends.

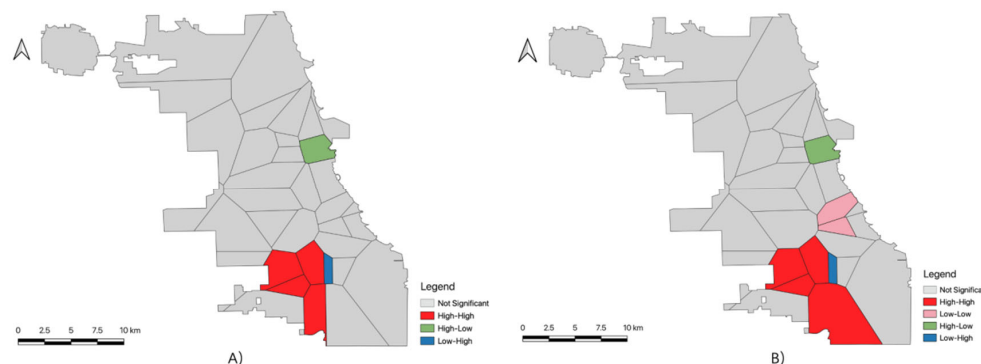


Figure 10. Clustering diagram of local Moran's I : (A) morning peak on weekdays; (B) evening peak on weekdays.

Table 6. Results of spatial correlation analysis.

Factor	Moran's <i>I</i>	<i>p</i> -Value
PD	−0.15	0.004
PA	−0.18	0.004
DBR	−0.10	0.08

In addition to spatial autocorrelation, spatial heterogeneity is another essential feature of sound distribution. We define spatial heterogeneity as the difference in sound magnitude between diverse regions of Chicago. The results of the factor detector are sorted by *q* value as follows: PA (0.2617) > PD (0.1975) > DS (0.1581) > DRN (0.1558) > DBR (0.1402) > NFS (0.0970) > NH (0.0722). Of the seven factors, NH and NFS have a small effect on sound levels, PA has the largest effect, and PD is a close second, indicating that PA and PD are the most important drivers of sound levels in Chicago. Due to the reduction effect of vegetation and lakes on sound in the park, the sound decreases with the increase in the park area. This further illustrates that the most central way to improve the future sound environment in Chicago is to increase vegetation cover and lake area. In addition, population distribution has an important effect on the spatial differentiation of sound levels. DS, DRN, and DBR also have a large effect on sound levels, suggesting that an important aspect of improving Chicago's sound environment is proper planning of the road network. The influence of NFS and NH on Chicago sounds are relatively small, which may be because hospitals have the need to keep quiet while fire stations produce a single sound.

The results of the interaction detector are shown below (Table 7). The interaction of the seven factors is enhanced, including bi-factor enhancement and nonlinear enhancement, and there are no factors that work independently of each other, which shows that the spatial differentiation pattern of the Chicago sounds is not controlled by a single factor but is the result of the joint action of multiple factors. The interaction between PD and PA (0.7353) as well as PA and DBR (0.6399) are significant in the interaction between the two factors, indicating that the population distribution should be intervened while the expansion of Chicago parks and investment in bike routes should be increased to jointly improve the noise distribution in Chicago. The interaction between NH and DRN (0.1740) as well as NH and NFS (0.1390) are small in the interaction between the two factors.

Table 7. The results of the interaction detector.

	PD	PA	DRN	DS	DBR	NH	NFS
PD	0.1975						
PA	0.7353 ^a	0.2617					
DRN	0.5377 ^a	0.4379 ^a	0.1558				
DS	0.4038 ^a	0.5435 ^a	0.4061 ^a	0.1581			
DBR	0.5797 ^a	0.6399 ^a	0.3219 ^a	0.3445 ^a	0.1402		
NH	0.2005 ^b	0.3312 ^b	0.1740 ^b	0.2892 ^a	0.4097 ^a	0.0722	
NFS	0.3714 ^a	0.3097 ^b	0.3194 ^a	0.4129 ^a	0.2528 ^a	0.1390 ^b	0.0970

Note: ^a represents that the interaction between the two factors is nonlinear enhancement; ^b means bi-factor enhancement.

7. Conclusions and Future Work

In this study, we analysed the sound environment in Chicago using sound data provided by the AoT. We examined the trend of the sound changes of each node in a week by drawing a line chart. The isolated sound nodes were divided into diverse regions using a Thiessen polygon, and the noise maps of various regions at different time periods were drawn using the geographic information system. The spatial distribution characteristics of sounds in Chicago and the influence of factors in space on the spatial distribution of sounds were explored by means of spatial correlation analysis and GeoDetector. Since the GeoDetector used in this study can detect the real interaction between two factors, it is

not limited to the multiplicative relationship, and the principle of GeoDetector ensures that it is immune to multi-independent variable collinearity, it achieves a more effective and comprehensive analysis. Taking the morning peak on weekdays as an example, we found that (1) there is a statistically significant positive correlation between noise in Chicago during this time. (2) Population density, park area, and density of bike routes were significantly negatively correlated with sound level. (3) Park area and population density are the two most crucial controlling factors for the spatial differentiation of sounds in Chicago. (4) There is an interaction enhancement effect between each factor, and the enhancement effects are more obvious between population density and park area as well as park area and density of bike routes. The results show that a good analysis result can also be achieved using AoT data. This study can provide a reference for Chicago's policy making and help Chicago to develop healthily and efficiently.

This study contributes to the study of urban sound. First, our study may be the first application of GeoDetector for Chicago's sound analysis. Compared to the previous literature that focused on the measurement of spatial autocorrelation, this study also focuses on the effects of urban factors on the spatial differentiation of sound. Second, this study enriches the research on noise pollution in Chicago, aids in better understanding the distribution of sounds in Chicago, provides suggestions for urban residents' travel, and offers the framework for the government to formulate relevant policies. Finally, we have used a Thiessen polygon to divide isolated sound nodes into different regions for research. This method is suitable for the study of any isolated points, such as sensors.

However, this study still has some limitations. The sound data only comes from 35 nodes, and the location of the sound nodes is not dense enough for the whole city. In addition, whether an individual identifies a sound as noise depends heavily on their specific activity and associated environment. Analysing the sound data collected by an urban sensor network can only explain a small number of troubles and distractions that people experience in their daily lives.

In the future, we will consider more aspects. First, we will consider historical data and use more data for analysis to support travel and government related decisions. Second, we will further adjust the weighted Thiessen polygon to empirically prove whether there will be a difference.

Author Contributions: Conceptualization, Jin Cheng and Shaohua Wang; Methodology, Jin Cheng and Shaohua Wang; Software, Yanjie Zhao and Shaohua Wang; Validation, Yanjie Zhao, Lei Qin, and Shaohua Wang; Writing—original draft, Yanjie Zhao and Xueyan Zhang; Writing—review and editing, Yanjie Zhao, Shaohua Wang, Jin Cheng, Lei Qin, and Xueyan Zhang. All authors have read and agreed to the published version of the manuscript.

Funding: This research was funded by the Natural Science Foundation of Beijing, grant numbers 4212036, Natural Science Foundation of China, grant numbers U2006218, 61901009, Concept Verification Project of Zhongguancun Open Laboratory, grant number 202005201-(07), Qin Xin Talents Cultivation Program, grant number QXTCP A202103, Beijing Key Laboratory for Sensors of BISTU, grant numbers E2U1050600, 2022CGKF00X, the Beijing Chaoyang District Collaborative Innovation Project (E2DZ050100), and Hundred Talents Program Youth Project (Category B) of the Chinese Academy of Sciences (E2Z10501).

Data Availability Statement: The AoT data were downloaded from <https://api.arrayofthings.org/> (accessed on 5 January 2022). The boundary data and street data were generated from <https://www.openstreetmap.org/> (accessed on 5 January 2022). The experimental data and codes can be obtained at: https://github.com/HIGISX/Chicago_Analytics_AOT.

Acknowledgments: The research was financially supported by the Hundred Talents Program Youth Project (Category B) of the Chinese Academy of Sciences (E2Z105010F).

Conflicts of Interest: The authors declare no conflict of interest.

Appendix A

There is a node that has a higher noise level throughout the week (Figure A1), and the overall noise level is higher than all other nodes. Among them, noise above 80.0 dB accounts for more than 76%, and noise above 90.0 dB accounts for more than 49%.

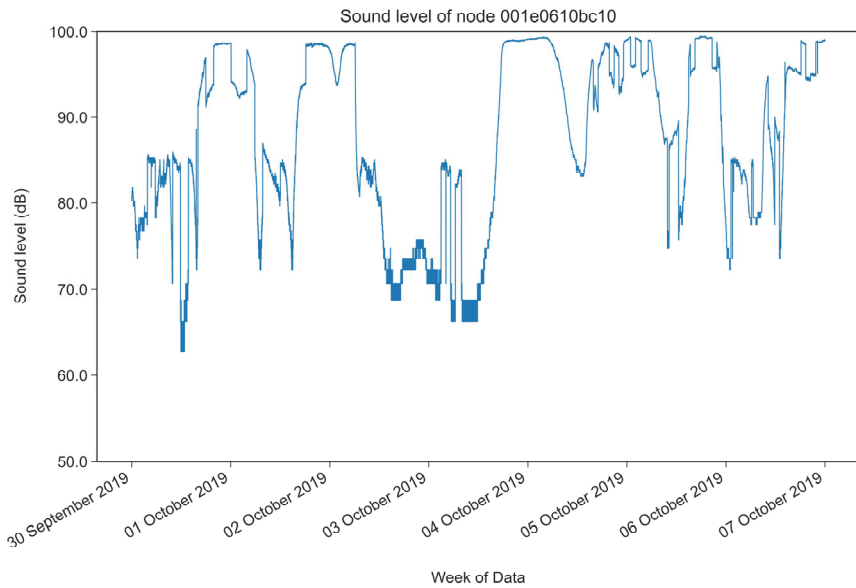


Figure A1. Sound level of node 001e0610bc10.

Appendix B

There are 13 nodes in total (Figures A2–A14). Despite the noise of the nodes being between 55.0 dB and 65.0 dB many times throughout the week, there were still several occasions when the noise was between 65.0 dB and 75.0 dB.

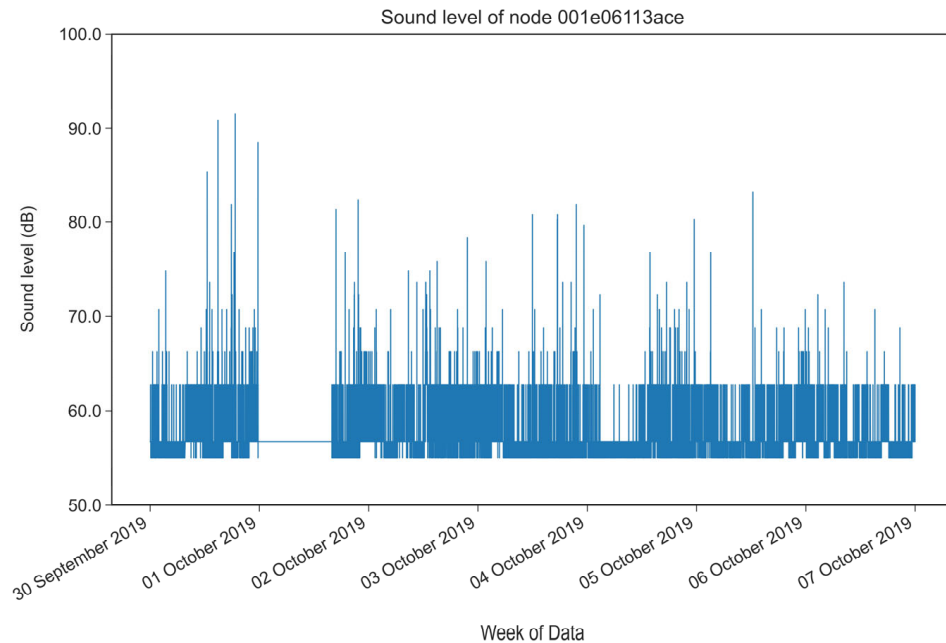


Figure A2. Sound level of node 001e06113ace.

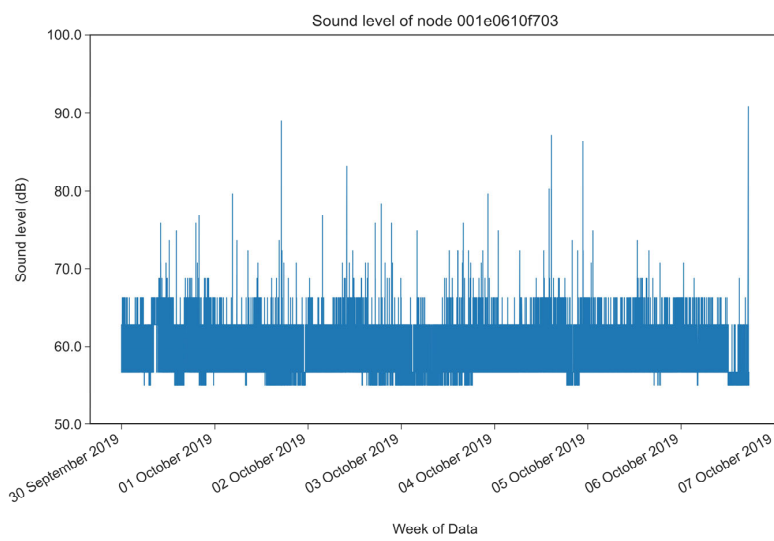


Figure A3. Sound level of node 001e0610f703.

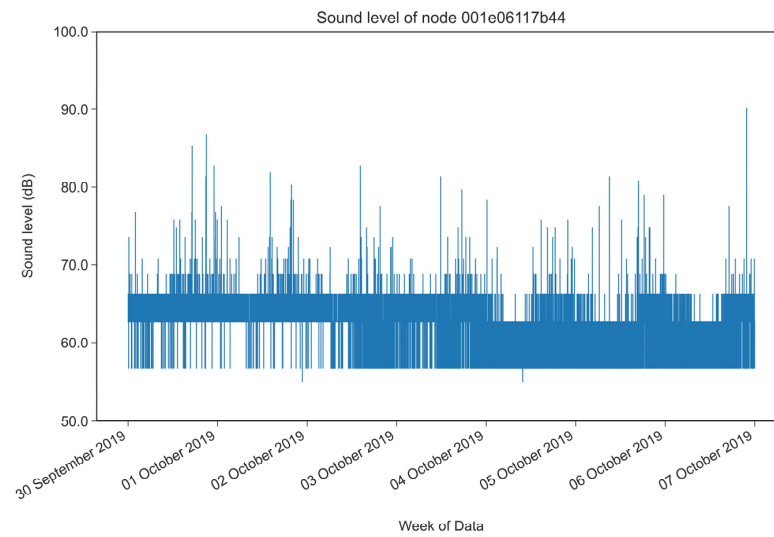


Figure A4. Sound level of node 001e06117b44.

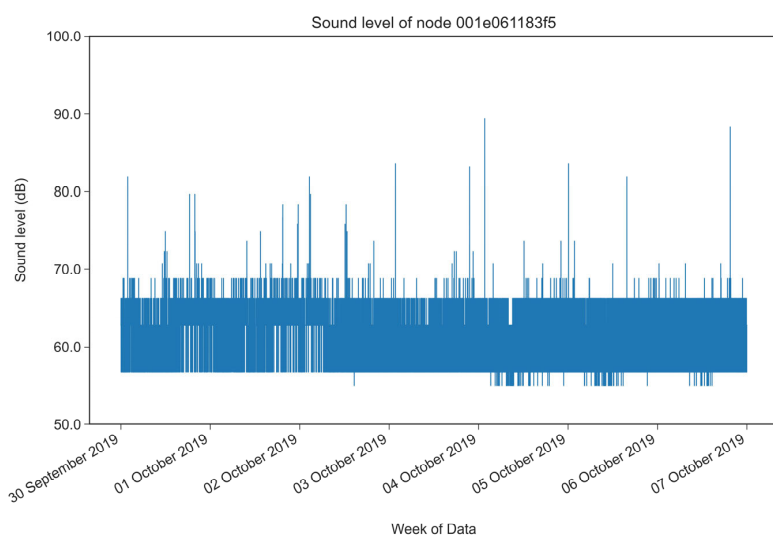


Figure A5. Sound level of node 001e061183f5.

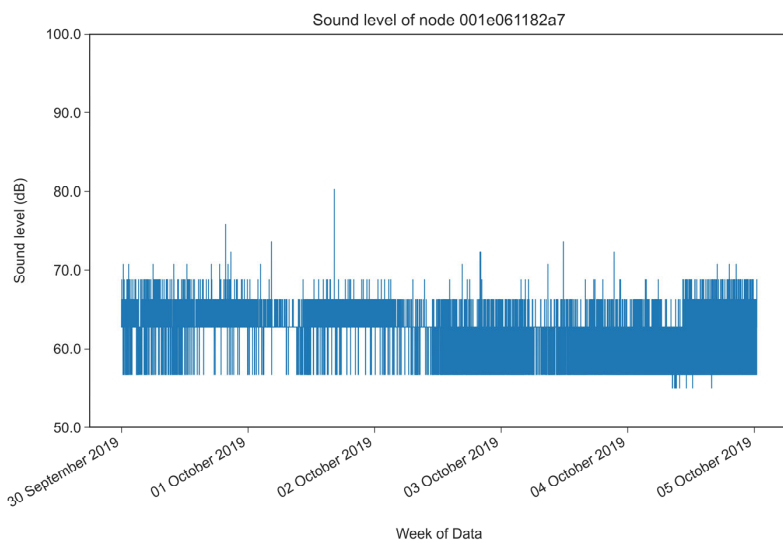


Figure A6. Sound level of node 001e061182a7.

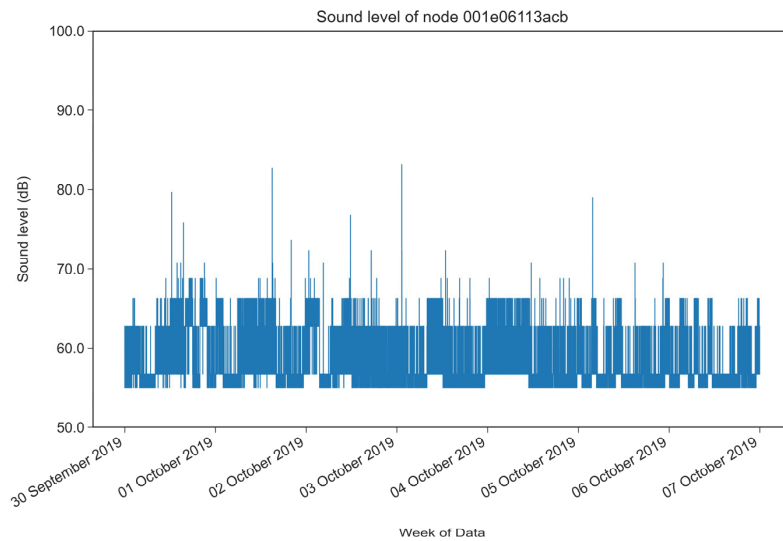


Figure A7. Sound level of node 001e06113acb.

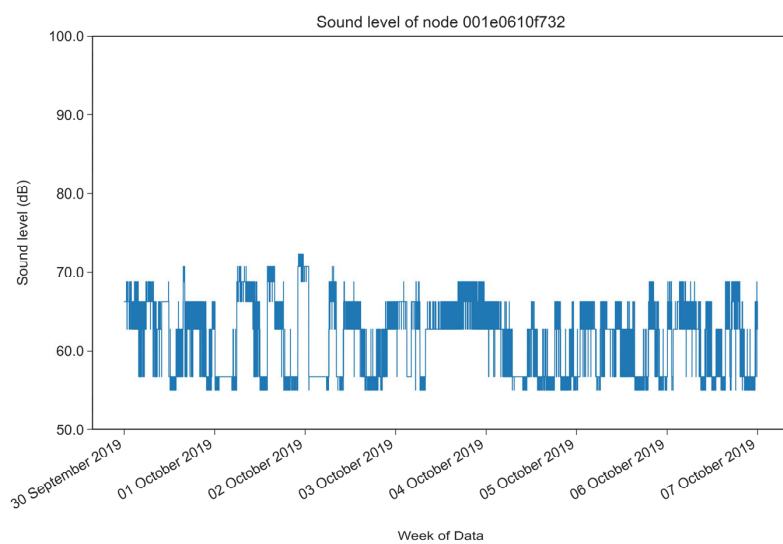


Figure A8. Sound level of node 001e0610f732.

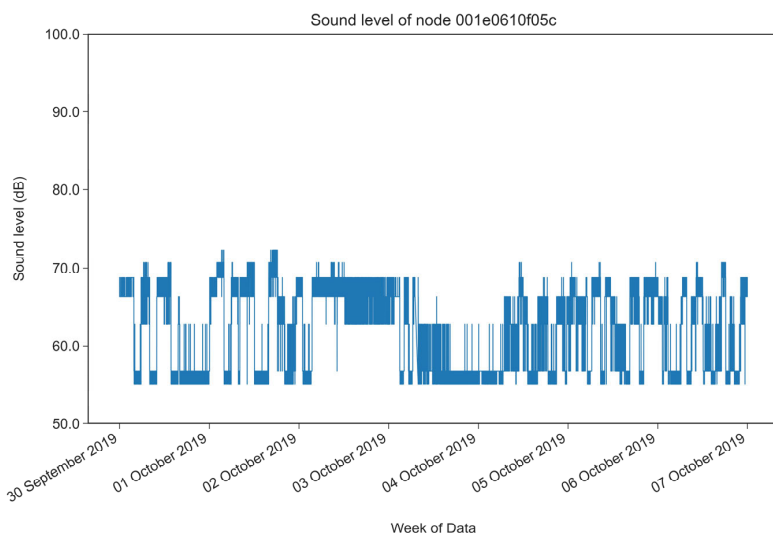


Figure A9. Sound level of node 001e0610f05c.

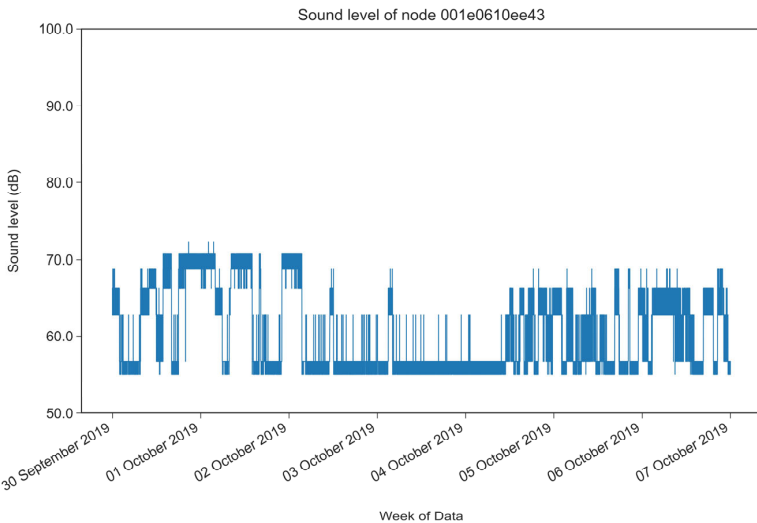


Figure A10. Sound level of node 001e0610ee43.

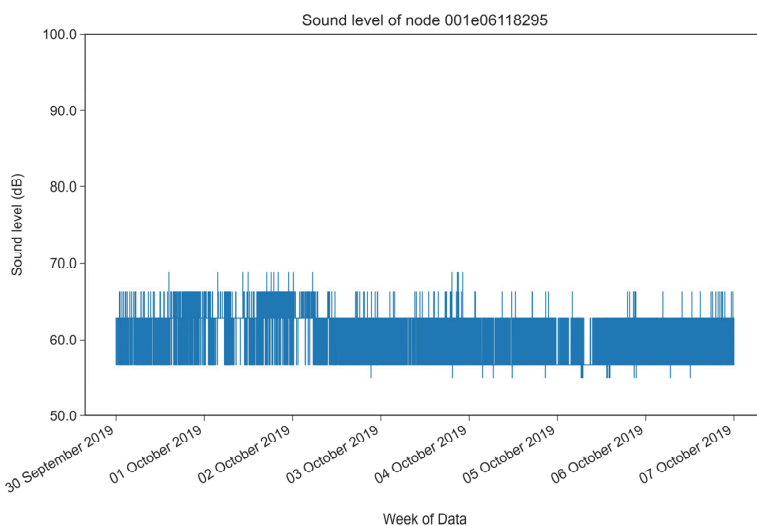


Figure A11. Sound level of node 001e06118295.

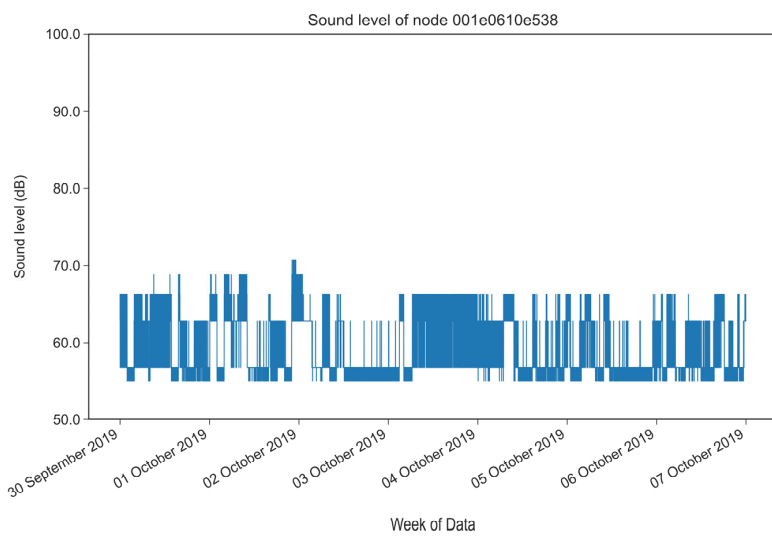


Figure A12. Sound level of node 001e0610e538.

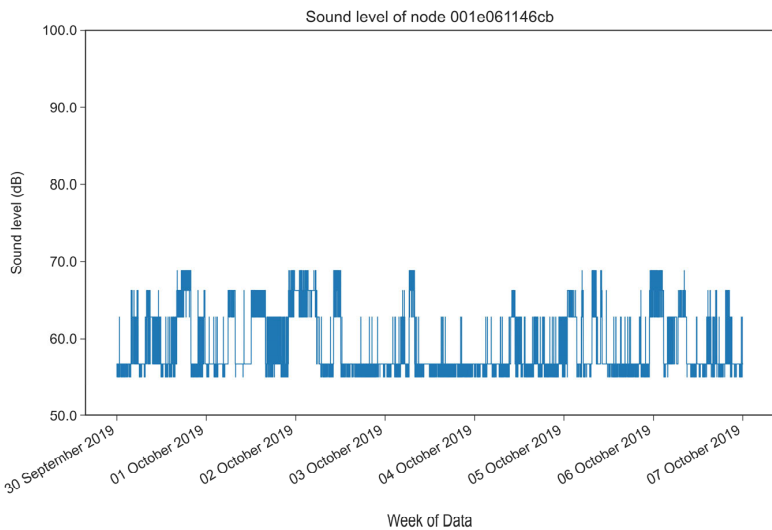


Figure A13. Sound level of node 001e061146cb.

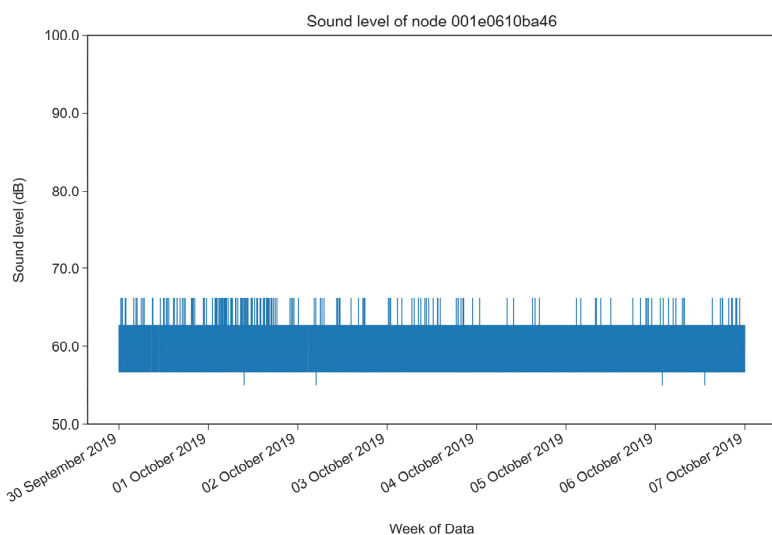


Figure A14. Sound level of node 001e0610ba46.

Appendix C

There are 14 nodes in total (Figures A15–A28). The noise of the nodes was between 55.0 dB and 65.0 dB most of the week, and sometimes, the noise exceeded 65.0 dB.

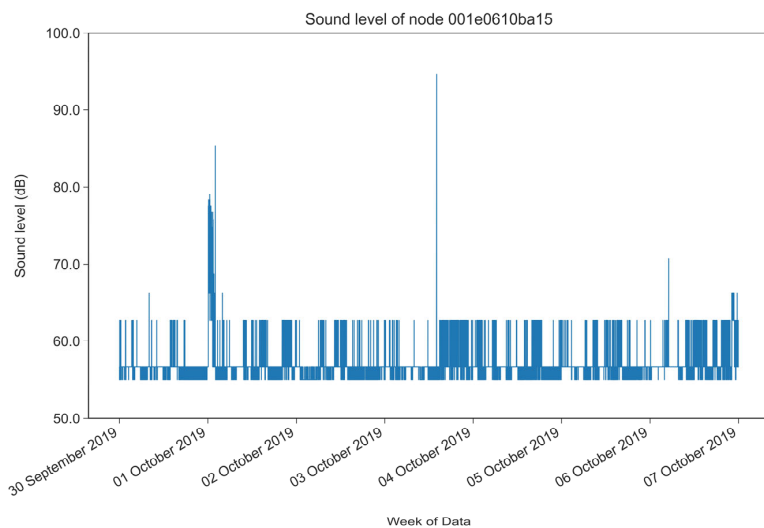


Figure A15. Sound level of node 001e0610ba15.

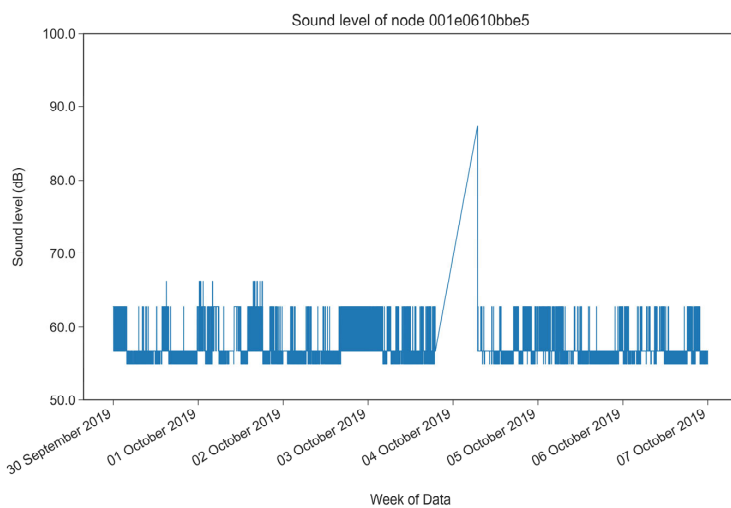


Figure A16. Sound level of node 001e0610bbe5.

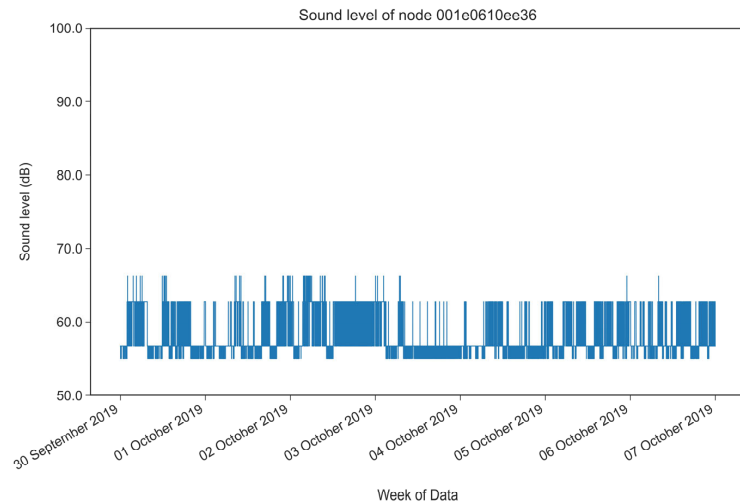


Figure A17. Sound level of node 001e0610ee36.

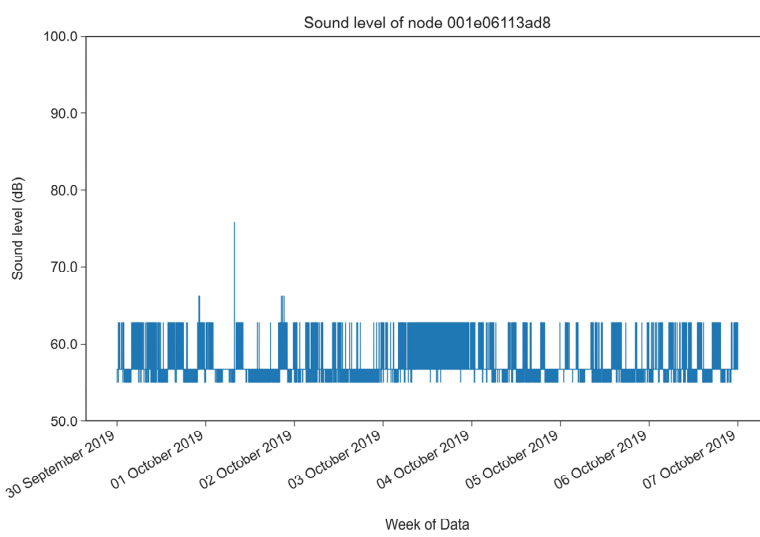


Figure A18. Sound level of node 001e06113ad8.

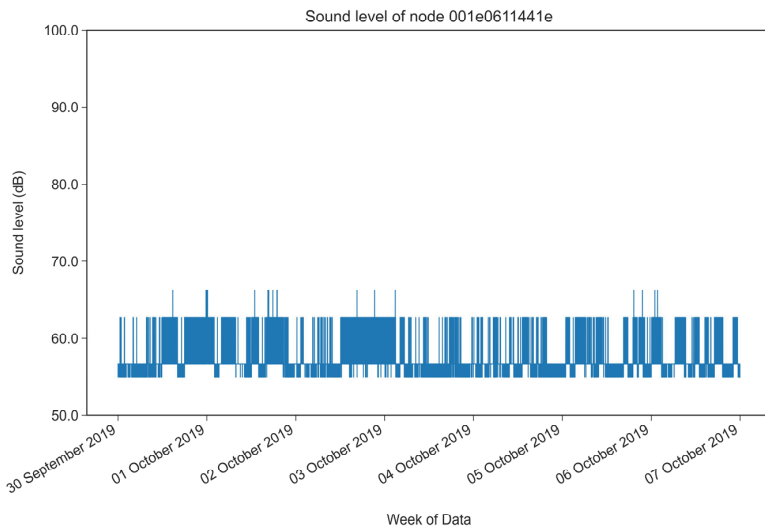


Figure A19. Sound level of node 001e0611441e.

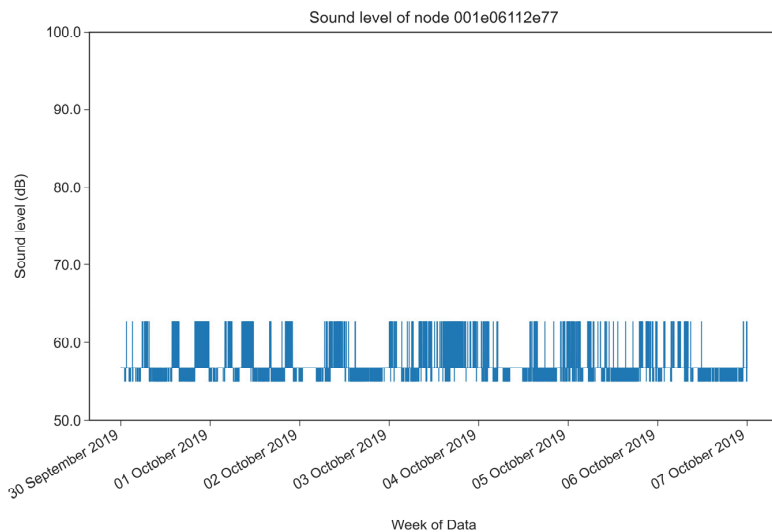


Figure A20. Sound level of node 001e06112e77.

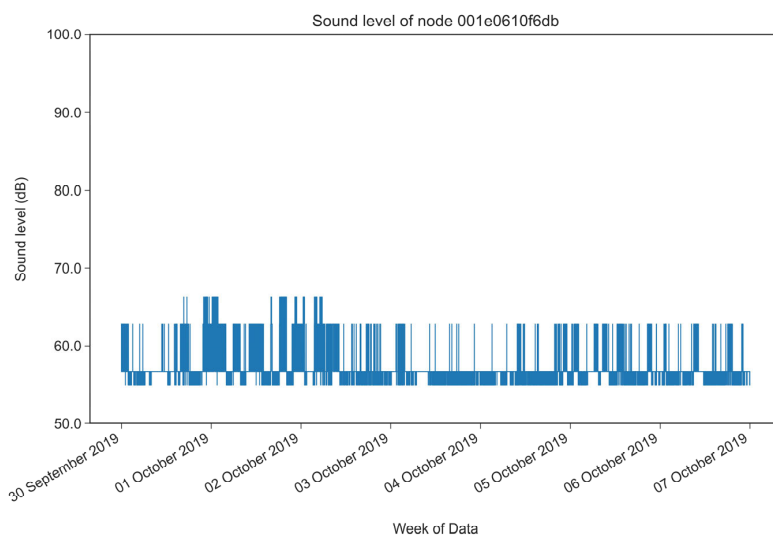


Figure A21. Sound level of node 001e0610f6db.

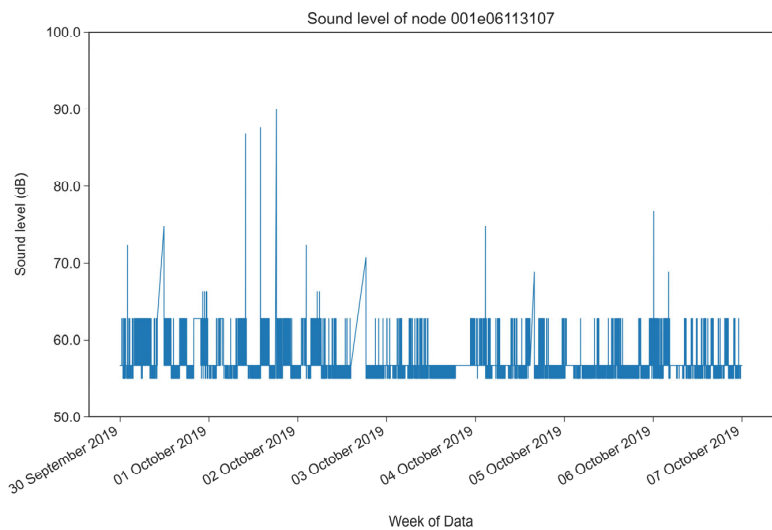


Figure A22. Sound level of node 001e06113107.

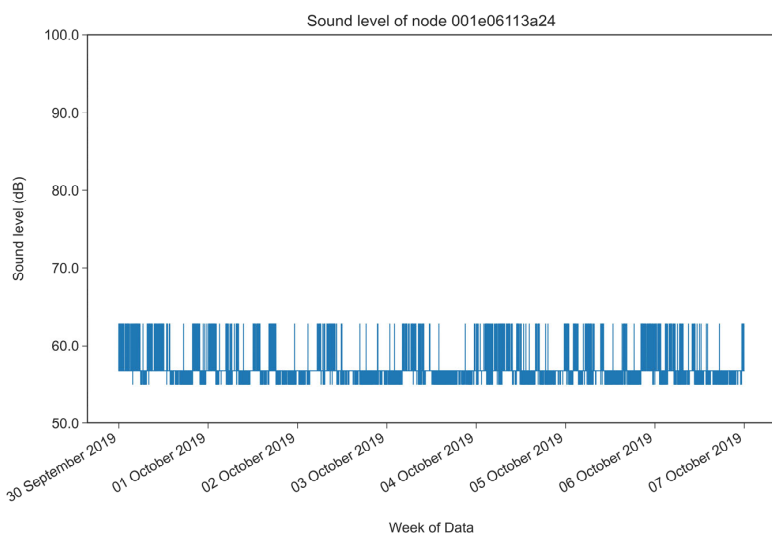


Figure A23. Sound level of node 001e06113a24.

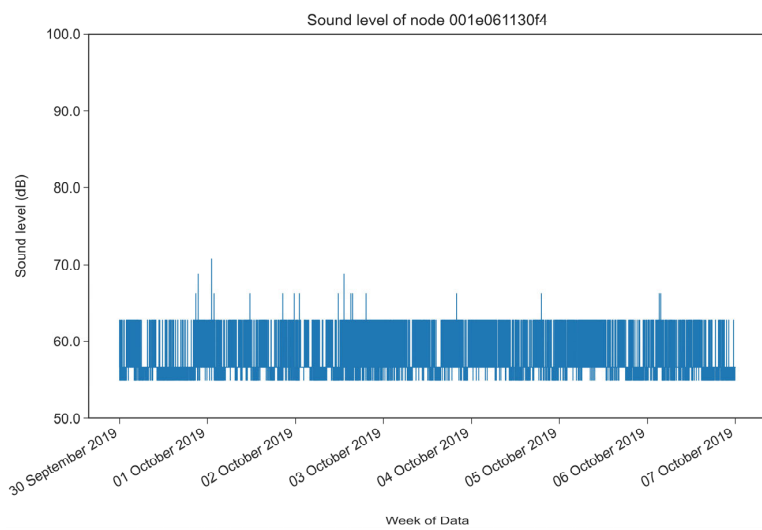


Figure A24. Sound level of node 001e061130f4.

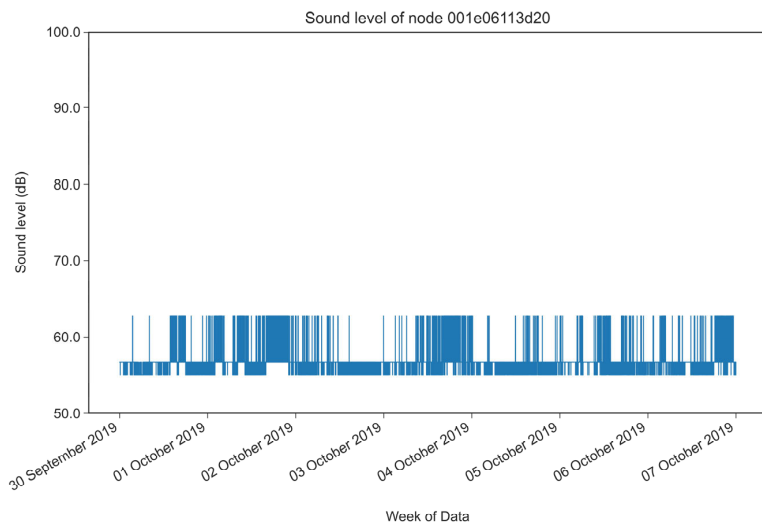


Figure A25. Sound level of node 001e06113d20.

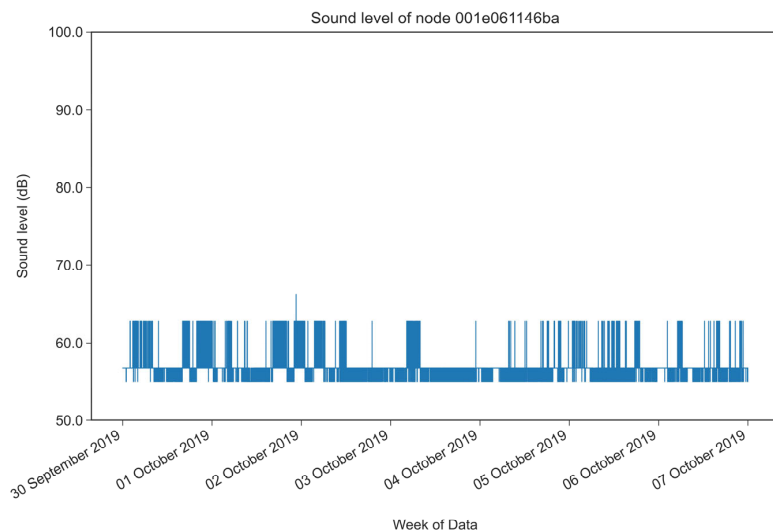


Figure A26. Sound level of node 001e061146ba.

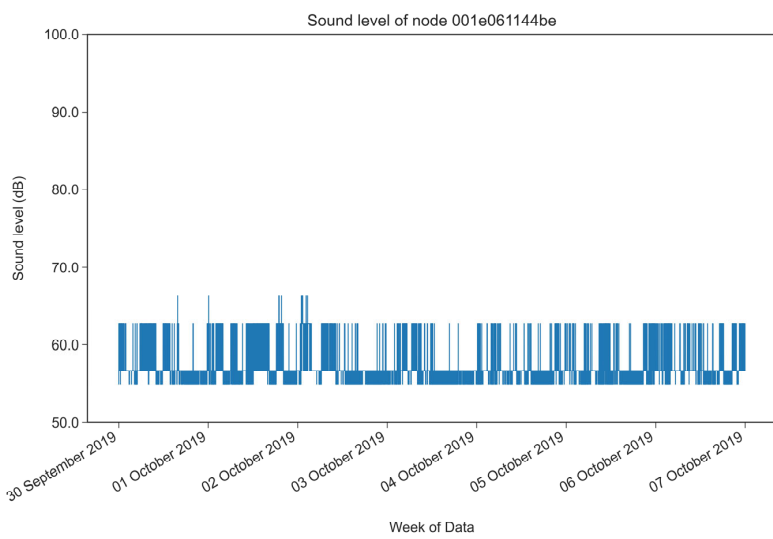


Figure A27. Sound level of node 001e061144be.

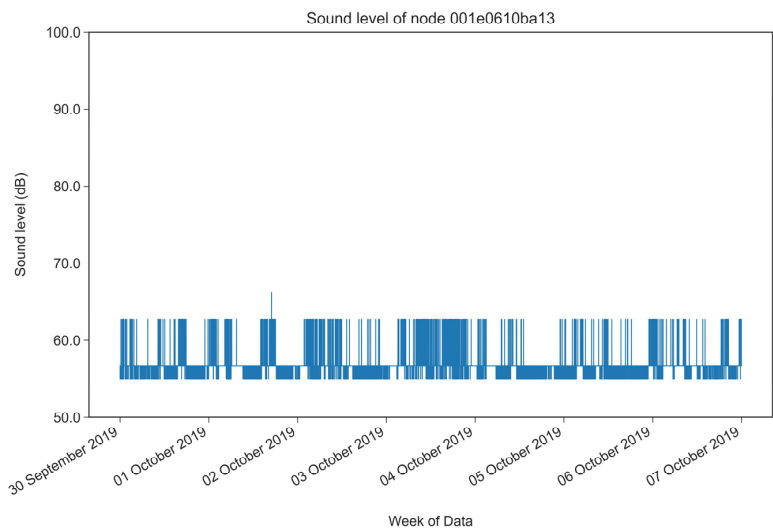


Figure A28. Sound level of node 001e0610ba13.

Appendix D

There are 7 nodes in total (Figures A29–A35). The node data were seriously missing, but its overall noise is between 55.0 dB and 67.5 dB.

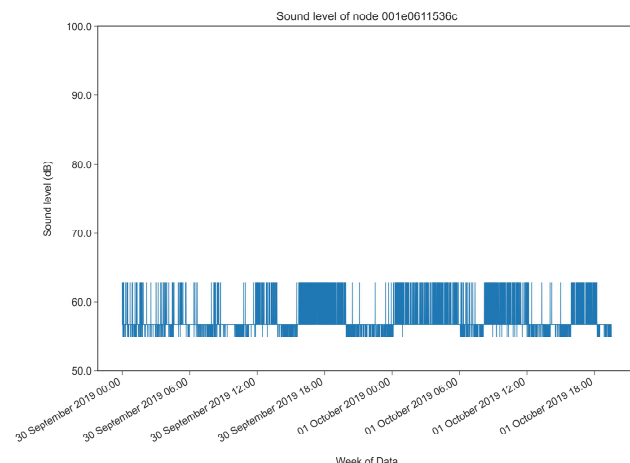


Figure A29. Sound level of node 001e0611536c.

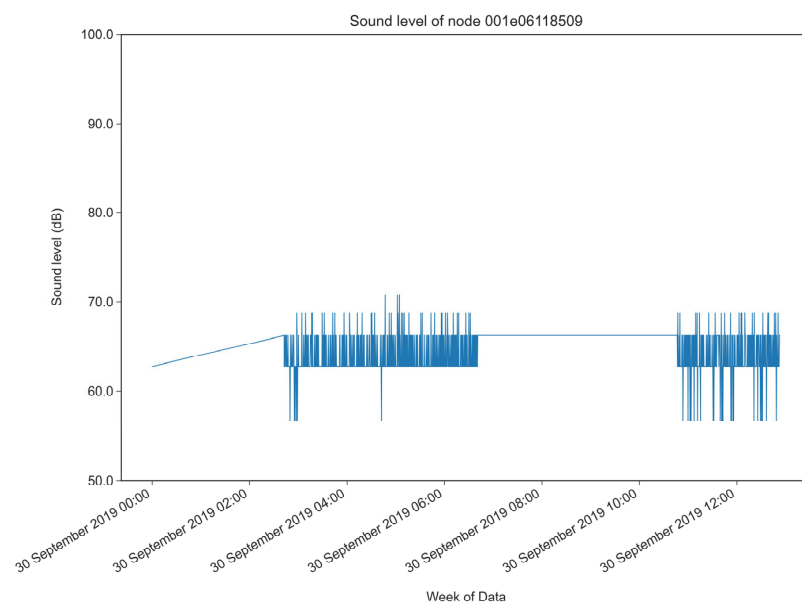


Figure A30. Sound level of node 001e06118509.

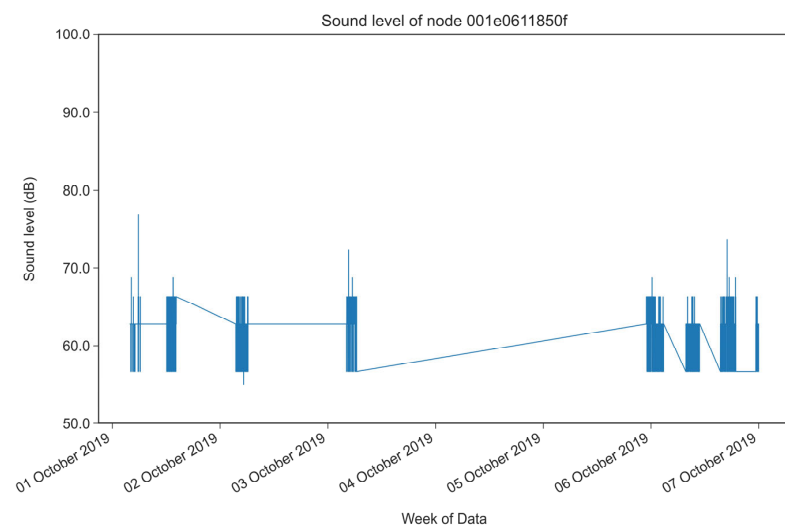


Figure A31. Sound level of node 001e0611850f.

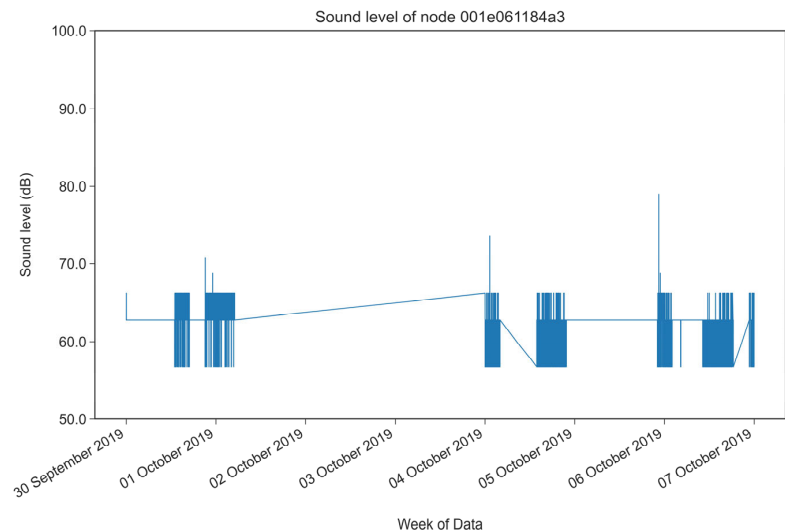


Figure A32. Sound level of node 001e061184a3.

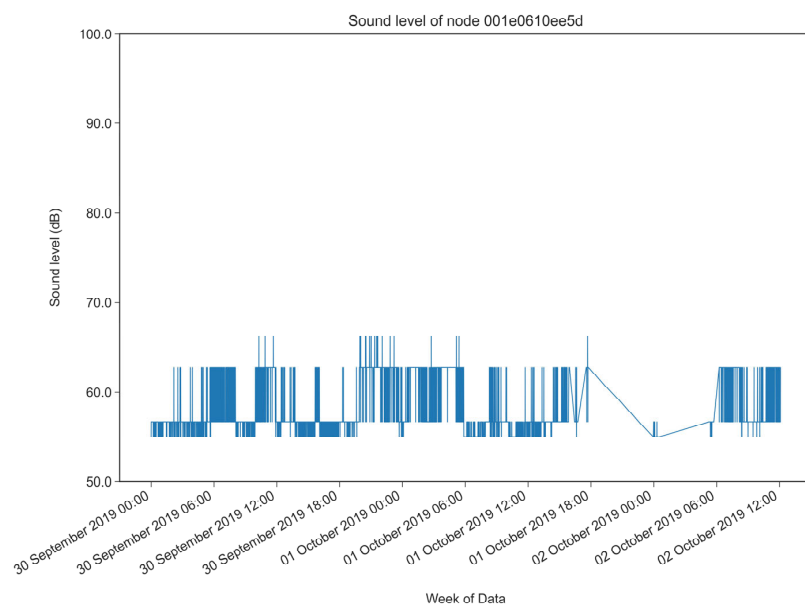


Figure A33. Sound level of node 001e0610ee5d.

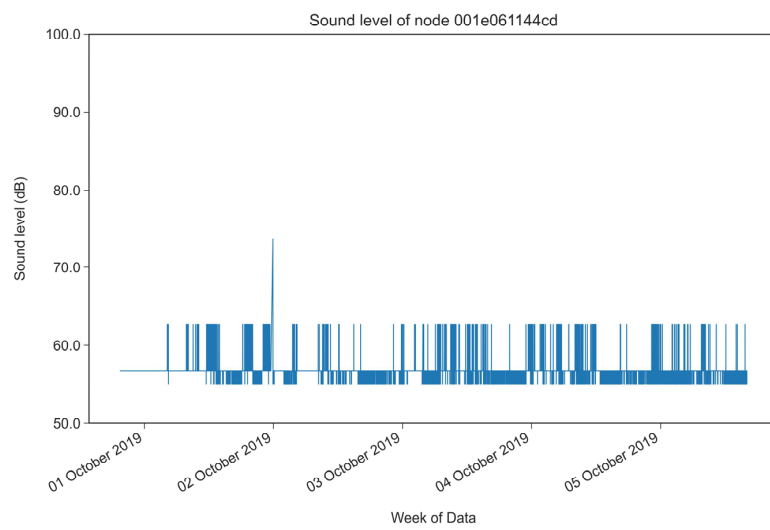


Figure A34. Sound level of node 001e061144cd.

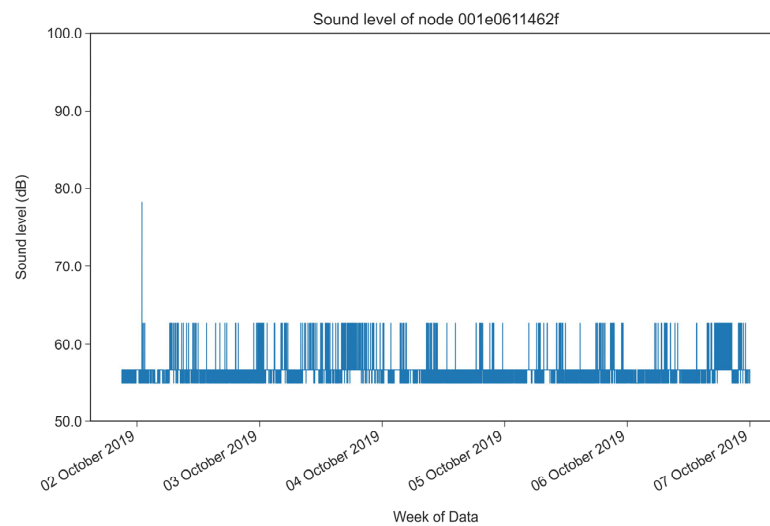


Figure A35. Sound level of node 001e0611462f.

References

- Caparros-Midwood, D.; Barr, S.; Dawson, R. Optimised spatial planning to meet long term urban sustainability objectives. *Comput. Environ. Urban Syst.* **2015**, *54*, 154–164. [[CrossRef](#)]
- Soliman, A.; Mackay, A.; Schmidt, A.; Allan, B.; Wang, S. Quantifying the geographic distribution of building coverage across the US for urban sustainability studies. *Comput. Environ. Urban Syst.* **2018**, *71*, 199–208. [[CrossRef](#)]
- King, E.A. Here, There, and Everywhere: How the SDGs Must Include Noise Pollution in Their Development Challenges. *Environ. Sci. Policy Sustain. Dev.* **2022**, *64*, 17–32. [[CrossRef](#)]
- Daniel, E. Noise and hearing loss: A review. *J. Sch. Health* **2007**, *77*, 225–231. [[CrossRef](#)] [[PubMed](#)]
- Klompmaker, J.O.; Hoek, G.; Bloemsma, L.D.; Wijga, A.H.; van den Brink, C.; Brunekreef, B.; Lebret, E.; Gehring, U.; Janssen, N.A.H. Associations of combined exposures to surrounding green, air pollution and traffic noise on mental health. *Environ. Int.* **2019**, *129*, 525–537. [[CrossRef](#)] [[PubMed](#)]
- Hao, G.; Zuo, L.; Xiong, P.; Chen, L.; Liang, X.; Jing, C. Associations of PM2.5 and road traffic noise with mental health: Evidence from UK Biobank. *Environ. Res.* **2022**, *207*, 112221. [[CrossRef](#)] [[PubMed](#)]
- Basner, M.; McGuire, S. WHO environmental noise guidelines for the European region: A systematic review on environmental noise and effects on sleep. *Int. J. Environ. Res. Public Health* **2018**, *15*, 519. [[CrossRef](#)] [[PubMed](#)]
- Münzel, T.; Sørensen, M.; Daiber, A. Transportation noise pollution and cardiovascular disease. *Nat. Rev. Cardiol.* **2021**, *18*, 619–636. [[CrossRef](#)]
- Bluhm, G.L.; Berglind, N.; Nordling, E.; Rosenlund, M. Road traffic noise and hypertension. *Occup. Environ. Med.* **2007**, *64*, 122–126. [[CrossRef](#)]
- Oftedal, B.; Krog, N.H.; Pyko, A.; Eriksson, C.; Graff-Iversen, S.; Haugen, M.; Schwarze, P.; Pershagen, G.; Aasvang, G.M. Road traffic noise and markers of obesity—A population-based study. *Environ. Res.* **2015**, *138*, 144–153. [[CrossRef](#)]
- Chen, H.L.; Koprowski, J.L. Animal occurrence and space use change in the landscape of anthropogenic noise. *Biol. Conserv.* **2015**, *192*, 315–322. [[CrossRef](#)]
- Catlett, C.E.; Beckman, P.H.; Sankaran, R.; Galvin, K.K. Array of things: A scientific research instrument in the public way: Platform design and early lessons learned. In Proceedings of the 2nd International Workshop on Science of Smart City Operations and Platforms Engineering, Pittsburgh, PA, USA, 18–21 April 2017; pp. 26–33. [[CrossRef](#)]
- Ricaurte, L. The array of things, Chicago. *Urban Plan. Transit.* **2021**, *171*–182. [[CrossRef](#)]
- Wang, S.; Lyu, F.; Wang, S.; Catlett, C.E.; Padmanabhan, A.; Soltani, K. Integrating CyberGIS and urban sensing for reproducible streaming analytics. In *Urban Informatics*; Springer: Singapore, 2021; pp. 663–681. [[CrossRef](#)]
- Lyu, F.; Wang, S.; Han, S.Y.; Catlett, C.; Wang, S. An integrated cyberGIS and machine learning framework for fine-scale prediction of urban Heat Island using satellite remote sensing and urban sensor network data. *Urban Inform.* **2022**, *1*, 6. [[CrossRef](#)] [[PubMed](#)]
- English, N.; Zhao, C.; Brown, K.L.; Catlett, C.; Cagney, K. Making sense of sensor data: How local environmental conditions add value to social science research. *Soc. Sci. Comput. Rev.* **2022**, *40*, 179–194. [[CrossRef](#)] [[PubMed](#)]
- Ruge, L.; Altakrouri, B.; Schrader, A. Sound of the City—Continuous noise monitoring for a healthy city. In Proceedings of the 2013 IEEE International Conference on Pervasive Computing and Communications Workshops (PERCOM Workshops), San Diego, CA, USA, 18–22 March 2013; pp. 670–675. [[CrossRef](#)]
- Wang, Y.; Zheng, Y.; Liu, T. A noise map of New York city. In Proceedings of the 2014 ACM International Joint Conference on Pervasive and Ubiquitous Computing: Adjunct Publication, Seattle, WA, USA, 13–17 September 2014; pp. 275–278. [[CrossRef](#)]
- Rendón, J.; Gómez, D.M.M.; Colorado, H.A. Useful tools for integrating noise maps about noises other than those of transport, infrastructures, and industrial plants in developing countries: Casework of the Aburra Valley, Colombia. *J. Environ. Manag.* **2022**, *313*, 114953. [[CrossRef](#)] [[PubMed](#)]
- Khan, J.; Ketzel, M.; Kakosimos, K.; Sørensen, M.; Jensen, S.S. Road traffic air and noise pollution exposure assessment—A review of tools and techniques. *Sci. Total Environ.* **2018**, *634*, 661–676. [[CrossRef](#)]
- Islam, M.N.; Rahman, K.S.; Bahar, M.M.; Habib, M.A.; Ando, K.; Hattori, N. Pollution attenuation by roadside greenbelt in and around urban areas. *Urban For. Urban Green.* **2012**, *11*, 460–464. [[CrossRef](#)]
- Van Renterghem, T.; Botteldooren, D.; Verheyen, K. Road traffic noise shielding by vegetation belts of limited depth. *J. Sound Vib.* **2012**, *331*, 2404–2425. [[CrossRef](#)]
- Ow, L.F.; Ghosh, S. Urban cities and road traffic noise: Reduction through vegetation. *Appl. Acoust.* **2017**, *120*, 15–20. [[CrossRef](#)]
- Yuan, M.; Yin, C.; Sun, Y.; Chen, W. Examining the associations between urban built environment and noise pollution in high-density high-rise urban areas: A case study in Wuhan, China. *Sustain. Cities Soc.* **2019**, *50*, 101678. [[CrossRef](#)]
- Han, X.; Huang, X.; Liang, H.; Ma, S.; Gong, J. Analysis of the relationships between environmental noise and urban morphology. *Environ. Pollut.* **2018**, *233*, 755–763. [[CrossRef](#)] [[PubMed](#)]
- Guo, L.H.; Cheng, S.; Liu, J.; Wang, Y.; Cai, Y.; Hong, X.-C. Does social perception data express the spatio-temporal pattern of perceived urban noise? A case study based on 3,137 noise complaints in Fuzhou, China. *Appl. Acoust.* **2022**, *201*, 109129. [[CrossRef](#)]
- Wang, H.; Chen, H.; Cai, M. Evaluation of an urban traffic Noise-Exposed population based on points of interest and noise maps: The case of Guangzhou. *Environ. Pollut.* **2018**, *239*, 741–750. [[CrossRef](#)] [[PubMed](#)]
- De Kluijver, H.; Stoter, J. Noise mapping and GIS: Optimising quality and efficiency of noise effect studies. *Comput. Environ. Urban Syst.* **2003**, *27*, 85–102. [[CrossRef](#)]

29. Cai, M.; Zou, J.; Xie, J.; Ma, X. Road traffic noise mapping in Guangzhou using GIS and GPS. *Appl. Acoust.* **2015**, *87*, 94–102. [[CrossRef](#)]
30. Lan, Z.; Cai, M. Dynamic traffic noise maps based on noise monitoring and traffic speed data. *Transp. Res. Part D Transp. Environ.* **2021**, *94*, 102796. [[CrossRef](#)]
31. Yang, W.; He, J.; He, C.; Cai, M. Evaluation of urban traffic noise pollution based on noise maps. *Transp. Res. Part D Transp. Environ.* **2020**, *87*, 102516. [[CrossRef](#)]
32. Yilmaz, G.; Hocanli, Y. Mapping of noise by using GIS in Şanlıurfa. *Environ. Monit. Assess.* **2006**, *121*, 103–108. [[CrossRef](#)]
33. Chiou, Y.C.; Jou, R.C.; Yang, C.H. Factors affecting public transportation usage rate: Geographically weighted regression. *Transp. Res. Part A Policy Pract.* **2015**, *78*, 161–177. [[CrossRef](#)]
34. Fang, S.; Zhao, Y.; Chao, Z.; Kang, X. Spatial Distribution Characteristics and Influencing Factors of Tibetan Buddhist Monasteries in Amdo Tibetan Inhabited Regions, China. *J. Geovisualiz. Spat. Anal.* **2022**, *6*, 29. [[CrossRef](#)]
35. Huang, Y.; Yan, Q.; Zhang, C. Spatial–temporal distribution characteristics of PM_{2.5} in China in 2016. *J. Geovisualiz. Spat. Anal.* **2018**, *2*, 12. [[CrossRef](#)]
36. Li, T. A Spatiotemporal Analysis of Rock Concerts Associated with Demographics and Leisure and Hospitality Employment. *J. Geovisualiz. Spat. Anal.* **2022**, *6*, 18. [[CrossRef](#)]
37. Li, X.; Xie, Y.; Wang, J.; Christakos, G.; Si, J.; Zhao, H.; Ding, Y.; Li, J. Influence of planting patterns on fluoroquinolone residues in the soil of an intensive vegetable cultivation area in northern China. *Sci. Total Environ.* **2013**, *458*, 63–69. [[CrossRef](#)]
38. Ren, Y.; Deng, L.; Zuo, S.; Luo, Y.; Shao, G.; Wei, X.; Hua, L.; Yang, Y. Geographical modeling of spatial interaction between human activity and forest connectivity in an urban landscape of southeast China. *Landsc. Ecol.* **2014**, *29*, 1741–1758. [[CrossRef](#)]
39. Zhu, L.; Meng, J.; Zhu, L. Applying Geodetector to disentangle the contributions of natural and anthropogenic factors to NDVI variations in the middle reaches of the Heihe River Basin. *Ecol. Indic.* **2020**, *117*, 106545. [[CrossRef](#)]
40. Luo, W.; Jasiewicz, J.; Stepinski, T.; Wang, J.; Xu, C.; Cang, X. Spatial association between dissection density and environmental factors over the entire conterminous United States. *Geophys. Res. Lett.* **2016**, *43*, 692–700. [[CrossRef](#)]
41. Zhao, R.; Zhan, L.; Yao, M.; Yang, L. A geographically weighted regression model augmented by Geodetector analysis and principal component analysis for the spatial distribution of PM2.5. *Sustain. Cities Soc.* **2020**, *56*, 102106. [[CrossRef](#)]
42. Xu, L.; Du, H.; Zhang, X. Driving forces of carbon dioxide emissions in China's cities: An empirical analysis based on the geodetector method. *J. Clean. Prod.* **2021**, *287*, 125169. [[CrossRef](#)]
43. Xinge, W.; Jianchao, X.; Dongyang, Y.; Tian, C. Spatial differentiation of rural touristization and its determinants in China: A geo-detector-based case study of Yesanpo Scenic Area. *J. Resour. Ecol.* **2016**, *7*, 464–471. [[CrossRef](#)]
44. Liao, Y.; Zhang, Y.; He, L.; Wang, J.; Liu, X.; Zhang, N.; Xu, B. Temporal and spatial analysis of neural tube defects and detection of geographical factors in Shanxi Province, China. *PLoS ONE* **2016**, *11*, e0150332. [[CrossRef](#)]
45. Wang, J.F.; Li, X.H.; Christakos, G.; Liao, Y.-L.; Zhang, T.; Gu, X.; Zheng, X.-Y. Geographical detectors-based health risk assessment and its application in the neural tube defects study of the Heshun Region, China. *Int. J. Geogr. Inf. Sci.* **2010**, *24*, 107–127. [[CrossRef](#)]
46. Wang, J.F.; Zhang, T.L.; Fu, B.J. A measure of spatial stratified heterogeneity. *Ecol. Indic.* **2016**, *67*, 250–256. [[CrossRef](#)]
47. Xu, D.; Zhang, K.; Cao, L.; Guan, X.; Zhang, H. Driving forces and prediction of urban land use change based on the geodetector and CA-Markov model: A case study of Zhengzhou, China. *Int. J. Digit. Earth* **2022**, *15*, 2246–2267. [[CrossRef](#)]
48. Huang, Y.K.; Mitchell, U.A.; Conroy, L.M.; Jones, R.M. Community daytime noise pollution and socioeconomic differences in Chicago, IL. *PLoS ONE* **2021**, *16*, e0254762. [[CrossRef](#)] [[PubMed](#)]
49. Mu, L. Thiessen polygon. In *International Encyclopedia of Human Geography*; Elsevier: Amsterdam, The Netherlands, 2009. [[CrossRef](#)]
50. Wang, S.; Sun, L.; Rong, J.; Yang, Z. Transit traffic analysis zone delineating method based on Thiessen polygon. *Sustainability* **2014**, *6*, 1821–1832. [[CrossRef](#)]
51. Dong, Z.; Bain, D.J.; Akcakaya, M.; Ng, C.A. Evaluating the Thiessen polygon approach for efficient parameterization of urban stormwater models. *Environ. Sci. Pollut. Res.* **2023**, *30*, 30295–30307. [[CrossRef](#)] [[PubMed](#)]
52. Widaningrum, D.L. A GIS-based approach for catchment area analysis of convenience store. *Procedia Comput. Sci.* **2015**, *72*, 511–518. [[CrossRef](#)]
53. Abeyrathna, W.; Langen, T.A. Effect of Daylight Saving Time clock shifts on white-tailed deer-vehicle collision rates. *J. Environ. Manag.* **2021**, *292*, 112774. [[CrossRef](#)]
54. Coate, D.; Markowitz, S. The effects of daylight and daylight saving time on US pedestrian fatalities and motor vehicle occupant fatalities. *Accid. Anal. Prev.* **2004**, *36*, 351–357. [[CrossRef](#)]
55. Meyerhoff, N.J. The influence of daylight saving time on motor vehicle fatal traffic accidents. *Accid. Anal. Prev.* **1978**, *10*, 207–221. [[CrossRef](#)]
56. Berglund, B.; Lindvall, T.; Schwela, D.H. New WHO guidelines for community noise. *Noise Vib. Worldw.* **2000**, *31*, 24–29. [[CrossRef](#)]
57. Zheng, Y.; Liu, T.; Wang, Y.; Zhu, Y.; Liu, Y.; Chang, E. Diagnosing New York city's noises with ubiquitous data. In Proceedings of the 2014 ACM International Joint Conference on Pervasive and Ubiquitous Computing, Seattle, WA, USA, 13–17 September 2014; pp. 715–725. [[CrossRef](#)]

58. Chen, Y.; Wang, S.; Yu, J.; Li, W.; Shi, X.; Yang, W. Optimal weighted voronoi diagram method of distribution network planning considering city planning coordination factors. In Proceedings of the 2017 4th International Conference on Systems and Informatics (ICSAI), Hangzhou, China, 11–13 November 2017; pp. 335–340. [[CrossRef](#)]
59. Sun, Y.; Wang, S.; Wang, Y. Estimating local-scale urban heat island intensity using nighttime light satellite imageries. *Sustain. Cities Soc.* **2020**, *57*, 102125. [[CrossRef](#)]
60. Ren, J.; Yang, J.; Zhang, Y.; Xiao, X.; Xia, J.C.; Li, X.; Wang, S. Exploring thermal comfort of urban buildings based on local climate zones. *J. Clean. Prod.* **2022**, *340*, 130744. [[CrossRef](#)]
61. Cohen, P.; Potchter, O.; Schnell, I. The impact of an urban park on air pollution and noise levels in the Mediterranean city of Tel-Aviv, Israel. *Environ. Pollut.* **2014**, *195*, 73–83. [[CrossRef](#)]
62. Monazzam, M.R.; Karimi, E.; Shahbazi, H.; Shahidzadeh, H. Effect of cycling development as a non-motorized transport on reducing air and noise pollution-case study: Central districts of Tehran. *Urban Clim.* **2021**, *38*, 100887. [[CrossRef](#)]

Disclaimer/Publisher's Note: The statements, opinions and data contained in all publications are solely those of the individual author(s) and contributor(s) and not of MDPI and/or the editor(s). MDPI and/or the editor(s) disclaim responsibility for any injury to people or property resulting from any ideas, methods, instructions or products referred to in the content.